ISTANBUL TECHNICAL UNIVERSITY ★ GRADUATE SCHOOL

SYNTHESIS AND CHARACTERIZATION OF UV-CURABLE AND CERAMIC SLURRY-LOADED EPOXY ACRYLATE RESIN FOR 3D PRINTING APPLICATION

M.Sc. THESIS

İrem Şeyma ÖZBALAK

Department of Polymer Science and Technology

Polymer Science and Technology Programme

JANUARY 2024

ISTANBUL TECHNICAL UNIVERSITY ★ GRADUATE SCHOOL

SYNTHESIS AND CHARACTERIZATION OF UV-CURABLE AND CERAMIC SLURRY-LOADED EPOXY ACRYLATE RESIN FOR 3D PRINTING APPLICATION

M.Sc. THESIS

İrem Şeyma ÖZBALAK
(515201001)

Department of Polymer Science and Technology

Polymer Science and Technology Programme

Thesis Advisor: Prof. Dr. Yeşim HEPUZER
Thesis Co-Advisor: Dr. Merve GÜRTEKİN SEDEN

JANUARY 2024

ISTANBUL TEKNİK ÜNİVERSİTESİ ★ LİSANSÜSTÜ EĞİTİM ENSTİTÜSÜ

3D BASKI UYGULAMASI İÇİN UV İLE KÜRLENEBİLEN VE SERAMİK BULAMAÇ YÜKLÜ EPOKSİ AKRİLAT REÇİNENİN SENTEZİ VE KARAKTERİZASYONU

YÜKSEK LİSANS TEZİ

İrem Şeyma ÖZBALAK
(515201001)

Polimer Bilim ve Teknolojisi Ana Bilim Dalı

Polimer Bilimi ve Teknolojisi Programı

Tez Danışmanı: Prof. Dr. Yeşim HEPUZER
Eş Danışman: Dr. Merve GÜRTEKİN SEDEN

OCAK 2024

İrem Şeyma ÖZBALAK, a M.Sc. student of İTU Graduate School student ID 515201001, successfully defended the thesis entitled "SYNTHESIS AND CHARACTERIZATION OF UV-CURABLE AND CERAMIC SLURRY-LOADED EPOXY ACRYLATE RESIN FOR 3D PRINTING APPLICATION", which she prepared after fulfilling the requirements specified in the associated legislations, before the jury whose signatures are below.

Thesis Advisor :	**Prof. Dr. Yeşim HEPUZER** İstanbul Technical University	.....
Co-advisor :	**Dr. Merve GÜRTEKİN SEDEN** TÜBİTAK	.....
Jury Members :	**Prof. Dr. Nilhan KAYAMAN APOHAN** Marmara University	.....
	Prof. Dr. Bahire Filiz ŞENKAL İstanbul Technical University	.....
	Prof. Dr. Nilgün KIZILCAN İstanbul Technical University	.....

Date of Submission : 28 December 2023
Date of Defense : 29 January 2024

To Efemu,

FOREWORD

Foremost, I would like to express my sincere gratitude to my esteemed supervisor, Prof. Dr. Yeşim HEPUZER, who provided her support and knowledge throughout my thesis studies, shared her valuable time with me, and always helped me with the research and writing of the thesis. I am honored to be her student during my master's degree education. I would like to express my appreciation to my thesis Co-advisor Dr. Merve GÜRTEKİN SEDEN for her guidance, endless motivation throughout my research and providing me the every opportunity to carry out my thesis. They also educated me on how to carry out scientific research, and they also contributed to develop myself in polymer science. This thesis would not have been possible without the support and encouragement of them. I feel very lucky to have met and worked with them.

I would like to express my gratitude to the esteemed Prof. Dr. Nilhan KAYAMAN APOHAN, Prof. Dr. Memet Vezir KAHRAMAN and Prof.Dr. Emrah ÇAKMAKÇI, who supported me throughout my undergraduate education and never failed to provide guidance throughout my master's degree.

I would like to express my most special thanks to my dear friends İrem DEMİR, Burhan BAŞEFE, Melisa AKSUN, Selen İrem ARMAĞAN, Melike ERTEM, Tuğçe AKBAL AYTAN, Emre AYTAN, Elif Mısra SERT, Barış Can BABAOĞLU, Mehmet KUTLUAY and Hande HIDIRLAR for all the support, morale and motivation they provided.

During all stages involved in the preparation of this thesis, I'm grateful to my family for their encouragement, understanding, patience and support all through my education.

Finally, I would like to express my most special thanks to my fiance, Efecan YAVAŞGEL, who never spared me his loving support and always made me feel it, and made me realize the strength within me when I had difficulties and lost faith in myself. Thank you for your endless support and inexhaustible tolerance during this difficult and tiring period of my life. My life has become much more meaningful with you.

I would like to thank The Scientific and Technological Research Council of Turkey (TUBITAK) (Project No: 20AG008) and PEGE Kimya, for financial and technical support.

January 2024 İrem Şeyma ÖZBALAK

(Chemist)

TABLE OF CONTENTS

Page

ABBREVIATIONS

3D : Three Dimensional
AM : Additive Manufacturing
BAPO : Phenylbis(2,4,6-trimethylbenzoyl)phosphine oxide
CAD : Computer Aided Design
CAS Number : Chemical Abstracts Service Number
Darocur 1173: 2-Hydroxy-2-methyl-1-phenyl-propan-1-one
DGEBA : Bisphenol A diglycidyl ether
DLP : Digital Light Processing
DSC : Differential Scanning Calorimetry
ECC : 3,4-Epoxycyclohexylmethyl 3,4- epoxycyclohexanecarboxylate
EtOH : Ethyl Alcohol
FDM : Fused Deposition Modelling
FTIR : Fourier-Transform Infrared Spectroscopy
HDDA : 1,6-Hexanediol Diacrylate
HQ : Hydroquinone
IPN : Interpenetrating Polymer Networks
PI : Photoinitiator
SEM : Scanning Electron Microscopy
SR355 : Di-trimethylolpropane Tetraacrylate
SLA : Stereolithography
SLS : Selective Laser Sintering
STL : Standard Tessellation language
TGA : Thermogravimetric Analysis
TPP : Triphenylphosphine
UV : Ultraviolet

SYMBOLS

cm	**:** Centimeter
cm^{-1}	**:** Reciprocal Centimeters
Eq	**:** Equivalent
F	**:** Factor
g	**:** Gram
Hz	**:** Hertz
h	**:** Hour
J	**:** Joule
kg	**:** Kilogram
L	**:** Liter
M	**:** Molarity
min	**:** Minute
ml	**:** Milliliter
mm	**:** Millimeter
mmol	**:** Millimole
MW	**:** Molecular Weight
nm	**:** Nanometer
N	**:** Normality
Pa·s	**:** Pascal-second
rpm	**:** Revolutions per minute
R	**:** Radical
Tg	**:** Glass Transition Temperature
Tm	**:** Melting Temperature
V	**:** Volume
v	**:** Frequency
W	**:** Watt
µm	**:** Micrometer
ΔH	**:** Enthalpy Change
°C	**:** Celcius
%	**:** Percent

LIST OF TABLES

Page

LIST OF FIGURES

Page

SYNTHESIS AND CHARACTERIZATION OF UV-CURABLE AND CERAMIC SLURRY-LOADED EPOXY ACRYLATE RESIN FOR 3D PRINTING APPLICATION

SUMMARY

The photochemical method to 3D printing is among the most alluring since it allows for the fabrication of items through photopolymerization processes involving monomers and oligomers, which has advantages for the environment, the economy, and manufacturing. In contrast to conventional methods, 3D printing uses a layer-by-layer approach to enable the advanced design and manufacture of complex 3D objects and structures while overcoming geometric restrictions. The utilization of liquid monomers and oligomers, which are systems that may cure or photopolymerize when exposed to a light source of a certain wavelength in the presence of a photoinitiator system, is the foundation of three-dimensional photopolymerization. The two most crucial elements of photopolymers for 3D printing in this method are monomers/oligomers and photoinitiators. In order to create the designed 3D items, photoinitiators absorb the irradiation light from a 3D printer and initiate the photopolymerization processes of monomers and oligomers layer by layer. Monomers and oligomers also determine the final qualities of the produced objects. It is vital to select a photoinitiator or photoinitiator system suitable for the selected monomer/oligomer structure and the mechanism used.

In this thesis, it is aimed to develop a novel product to be used in 3D printing technology. Studies were carried out on the resin system with ultraviolet light curable organic-inorganic hybrid structure to be used in 3D printing technology. Experimental parts that were carried out during the thesis work can be summarized in three main sections.

First of all, epoxy acrylate resin was synthesized to create the organic part of the material. Resin was obtained as a result of a reaction lasting 4 hours at 80 °C, using bisphenol A type epoxy resin and acrylic acid, hydroquinone as inhibitor and triphenylphosphine as catalyst. This synthesized epoxy acrylate resin was characterized by Fourier-Transform Infrared Spectroscopy (FTIR) analysis.

Secondly, a total of 30 grams of ceramic powder mixture was prepared to create the inorganic part of the material, including 80% silica powder with a particle size of 6.5 - 8.7 microns, 15% zirconia powder with a particle size of 5 microns, and 5% aluminum oxide powder with a particle size of 0.5 microns. The prepared ceramic powder mixture was mixed with the help of a turbula for 1 hour. Then, the resulting homogeneous powder mixture and ethanol were mixed to obtain a slurry. The prepared slurry was ground in a planetary ball mill at 300 rpm for 5 hours with the help of

zirconia balls. Particle size analysis of this ceramic mixture was performed with a mastersizer device.

Finally, by preparing these organic and inorganic structures and combining them with varying amounts of additive chemicals, 5 different samples were obtained. For each sample, together with 10 g of Epoxy acrylate resin, 20% by weight HDDA (1,6 hexanediol diacrylate) as reactive diluent, 0%, 30%, 40% and 50% by weight ceramic powder, 3% by weight dispersant, SR355, which is a tetraacrylate type, 5% by weight of crosslinker, 3% by weight of Darocur 1173 used as UV photoinitiator system, and 0.5% by weight of BAPO, respectively, were added. The prepared samples were cast in Teflon™ mold and prevented oxygen inhibition before curing. At the end of the process, the samples were cured with a high-pressure UV lamp (OSRAM, 300 W) for 180 seconds.

In conclusion; The thesis study was completed with the development of a unique material known as "green body" to be used in 3D printing technology. Materials containing different proportions of inorganic particles were analyzed comparatively with each other. Thermal properties were examined using Thermogravimetric analysis (TGA) and Differential Scanning Calorimetry (DSC), and morphological properties were examined using Scanning Electron Microscope (SEM).

3D BASKI UYGULAMASI İÇİN UV İLE KÜRLENEBİLEN VE SERAMİK BULAMAÇ YÜKLÜ EPOKSİ AKRİLAT REÇİNENİN SENTEZİ VE KARAKTERİZASYONU

ÖZET

3D baskıya yönelik fotokimyasal yöntem, çevre, ekonomi ve üretim açısından avantajlara sahip olan monomerleri ve oligomerleri içeren fotopolimerizasyon işlemleri yoluyla yeni ürünlerin üretilmesine olanak tanıdığı için oldukça çekici yöntemlerden biridir. Geleneksel yöntemlerin aksine, 3D baskıda, geometrik kısıtlamaların üstesinden gelirken karmaşık 3D nesnelerin ve yapıların gelişmiş tasarımını ve üretimini mümkün kılmak için katman katman bir yaklaşım kullanılır. Üç boyutlu (3D) baskı, bilgisayar destekli tasarım (CAD) kullanımıyla, polimer gibi farklı malzemelerin üst üste konularak kalıplara ihtiyaç duymadan ürün oluşturulmasını sağlayan bir eklemeli imalat tekniğidir.

Bir fotobaşlatıcı sistem varlığında belirli bir dalga boyundaki ışık kaynağına maruz bırakıldığında sertleşebilen veya fotopolimerleşebilen sistemler olan sıvı monomer ve oligomerlerin kullanılması, üç boyutlu fotopolimerizasyonun temelini oluşturur. 3D Fotopolimerizasyona geniş bir perspektiften bakıldığında bu yaklaşım sürecinde dikkat edilmesi gereken noktaları dört ana kategoriye ayırmak mümkündür. Bu kategoriler mekanizmalar, teknikler, fotobaşlatıcılar ve dolgu malzemeleri olarak tanımlanabilir.

Bu yaklaşımda seçilen monomer/oligomerlerin hangi mekanizma ile ilerleyeceği ve monomer/oligomerlerin bu mekanizmaya uyumu son derece önemlidir. Seçilen monomer ve oligomerlerin türüne bağlı olarak fotokimyasal reaksiyon, serbest radikal mekanizması, katyonik mekanizma, ikili kürleme mekanizması veya tiyolen mekanizması yoluyla değişiklik gösterebilir. Monomerler ve oligomerler aynı zamanda üretilen nesnelerin nihai niteliklerini de belirler.

Seçilen monomer/oligomer yapısına ve kullanılan mekanizmaya uygun bir fotobaşlatıcı veya fotobaşlatıcı sisteminin seçilmesi hayati önem taşımaktadır. Tasarlanan 3 boyutlu öğeleri oluşturmak için foto başlatıcılar, 3 boyutlu yazıcıdan gelen ışınlama ışığını emer ve monomerlerin ve oligomerlerin katman katman fotopolimerizasyon süreçlerini başlatır. Bu mekanizmalara uygun, ticari olarak temin edilebilen birçok fotobaşlatıcı sistem bulunmaktadır.

Stereolitografi (SLA), Dijital Işık İşleme (DLP), Eriyik Biriktirmeli Modelleme (FDM) ve Seçici Lazer Sinterleme (SLS) dahil olmak üzere 3 boyutlu fotopolimerizasyona dayalı teknikler, kontrol edilebilir optik, kimyasal ve mekanik özelliklere sahip karmaşık çok işlevli malzeme sistemlerinin üç boyutlu olarak üretilmesini mümkün kılar. Bu yaklaşımlar aynı zamanda düşük özellik boyutlarıyla yüksek çözünürlük elde etmek için de kullanılabilir. Bu amaçla biyomedikal cihazlar,

cerrahi, diş hekimliği, mikroakışkanlar, ilaç dağıtımı, yumuşak robotik ve doku mühendisliği dahil olmak üzere çeşitli endüstrilerde yeni yollar bu teknoloji ile mümkün kılınmıştır.

Vat Fotopolimerizasyonu, sıvı fotopolimer reçinesinin ışık kullanılarak katman katman seçici olarak sertleştirilmesi prensibiyle çalışan bir 3 boyutlu baskı tekniğidir. Vat fotopolimerizasyonu, boyutsal hassasiyet açısından en önemli Eklemeli Üretim (AM) yaklaşımı olarak kabul edilmektedir, çünkü bu işlem, mikrometre aralığına kadar büyük çözünürlüklere, düşük toleranslara ve yüksek yüzey kalitesine sahip parçalar üretebilmektedir. Monomerler, fotobaşlatıcılar ve seramik tozundan oluşan süspansiyonun hazırlanması, seramiklerin Vat fotopolimerizasyonunda çok önemli bir adımdır. Diğer eklemeli üretim yöntemlerinden farklı olarak, Vat Fotopolimerizasyonu, bir fıçı içindeki sıvı reçine rezervuarıyla başlar. Vat Fotopolimerizasyonunun iki ana türü vardır. Bunlar, Stereolitografi (SLA) ve Dijital Işık İşleme (DLP) olarak adlandırılır. Her iki yöntem de sıvı reçineyi ışıkla sertleştirme temel ilkesini paylaşıyor ancak yaklaşımları birbirinden farklıdır. Dijital Işık İşleme tekniği ve Stereolitografi tekniği arasındaki temel fark ışık kaynağıdır; Stereolitografi tekniği bir UV lazer ışını kullanırken Dijital Işık İşleme tekniği bir projektörden gelen UV ışığını kullanır.

3D baskı teknolojisinde seramik, metal, kompozit, biyomalzemeler gibi birçok dolgu malzemesinden bahsetmek mümkündür. 3D baskıda seramik tozu kullanılacaksa; işlem, ışık kullanılarak sıvı reçine katmanının katman katman seçici olarak katılaştırılmasını içerir. Reçinedeki seramik dolgular, ince detaylandırma ve sağlam yapısal bütünlüğün ayırt edici bir kombinasyonunu sunar. Seramikler ince yapılara sahip olduklarından karmaşık yapıların oluşmasına olanak sağlarlar. Aynı zamanda üstün mukavemetleri ve aşınmaya karşı dirençleri ile bilindiklerinden mukavemet ve dayanıklılık sağlarlar.Seramikler yüksek sıcaklıklara ve çeşitli kimyasallara karşı mükemmel dirence sahiptir.Bu nedenle zorlu ortamlarda kullanım alanları geniştir.

Bu tez çalışmasında 3 boyutlu baskı teknolojisinde kullanılacak yeni bir ürünün geliştirilmesi amaçlanmaktadır. 3 boyutlu baskı teknolojisinde kullanılacak ultraviyole ışıkla kürlenebilen organik-inorganik hibrit yapıya sahip reçine sistemi üzerinde çalışmalar yapılmıştır. Tez çalışması sırasında gerçekleştirilen deneysel kısımlar üç ana bölümde özetlenebilir.

Öncelikle malzemenin organik kısmını oluşturmak için epoksi akrilat reçinesi sentezlendi. Bisfenol A tipi epoksi reçine ve akrilik asit, inhibitör olarak hidrokinon ve katalizör olarak trifenilfosfin kullanılarak, 80 °C'de 4 saat süren bir reaksiyon sonucunda reçine elde edildi. Sentezlenen bu epoksi akrilat reçinesi, Fourier-Transform Kızılötesi Spektroskopisi (FTIR) analizi ile karakterize edildi.

Daha sonra malzemenin inorganik kısmını oluşturmak için Partikül büyüklüğü 6,5 - 8,7 mikron olan ağırlıkça %80 silika tozu, 5 mikron partikül büyüklüğü olan ağırlıkça %15 zirkonya tozu ve 0,5 mikron partikül büyüklüğü olan ağırlıkça %5 alüminyum oksit tozu olmak üzere toplam 30 gram seramik tozu karışımı hazırlandı. Hazırlanan seramik tozu karışımı turbula yardımıyla 1 saat karıştırıldı. Daha sonra elde edilen homojen toz karışımı distile su ve etanol karıştırılıp bir bulamaç elde edildi. Hazırlanan bulamaç, zirkon topları yardımı ile planeter bilyeli değirmende 300 rpm'de 5 saat boyunca öğütüldü. Bu seramik karışımının partikül boyutu analizi mastersizer cihazı ile yapıldı.

Son olarak, bu organik ve inorganik yapıların hazırlanması sonucu değişen miktarlarda katkı kimyasallarıyla birleştirilmesi ile birlikte 5 adet yeşil gövde numunesi

hazırlanmıştır. Her numune için 10 gr Epoksi akrilat reçinesi ile birlikte, sırasıyla, reaktif seyreltici olarak ağırlıkça %20 HDDA (1,6 heksandiol diakrilat), ağırlıkça %0, %30, %40 ve %50 oranında seramik tozu, ağırlıkça %3 oranında dispersant, tetraakrilat türü olan SR355, ağırlıkça %5'i oranında çapraz bağlayıcı, UV fotobaşlatıcı sistem olarak kullanılan ağırlıkça %3 oranında Darocur 1173 ve ağırlıkça %0,5 oranında BAPO eklendi. Hazırlanan numunelerin kürlenmesi için; 5 bölmeye sahip, bölmelerin boyutları 50 mm x 10 mm x 1 mm olan özel bir Teflon kalıp tasarlanıp yaptırıldı ve numuneler bu kalıba döküldü. Kürleme işleminden önce oksijen inhibisyonunu önlendi. Hazırlanıp Teflon kalıba dökülen organik-inorganik hibrit formülasyonları UV ile kürlemek için UV kabine yerleştirildi. Teflon kalıpla UV ışık kaynağı arasına standart bir mesafe konulup kürleme işlemi başlatıldı. Sistemde UV ışık kaynağı olarak yüksek basınçlı UV lambası (OSRAM, 300W) kullanılmıştır. Numuneler yüksek basınçlı UV lambası ile 180 saniye süreyle kürlendi. Hazırlanan numuneler seramik oranları baz alınarak EAC0, EAC30, EAC40, EAC50 olarak isimlendirilmişlerdir.

Farklı oranlarda inorganik madde içeren malzemeler birbirleriyle karşılaştırmalı olarak analiz edildi. Sentezlenen epoksi akrilat reçinesi, Fourier-Transform Kızılötesi Spektroskopisi (FTIR) ile karakterize edilmiştir. Termal özellikler Termogravimetrik analiz (TGA) ve Diferansiyel Taramalı Kalorimetre (DSC) kullanılarak, morfolojik özellikler ise Taramalı Elektron Mikroskobu (SEM) kullanılarak incelenmiştir.

Sonuç olarak tüm verileri değerlendirdiğimizde; 3 boyutlu baskı teknolojisinde kullanılmak üzere "yeşil gövde" olarak bilinen benzersiz bir malzemenin geliştirilmesiyle tez çalışması tamamlandı. Epoksi akrilat reçinesi ile hazırlanıp seramik tozu ve diğer kimyasallarla desteklenip kürlenen bu yeni malzeme, UV ile kürlenebilen inorganik organik hibrit yapıya sahip olup, 3D baskı teknolojisinde kullanıma uygun olduğunu göstermektedir.

1. INTRODUCTION

Three-dimensional (3D) printing, with the use of computer-aided design (CAD), is an additive manufacturing technique that enables the creation of products without the need of molds by layering different materials, such as polymers, on top of one another [1–3]. In the 1980s, 3D printing technologies were developed with the aim of fabricating complicated or personalized products without the need of molds or machining [2,4]. Novel applications in rapid prototyping, dentistry, biomedical devices, tooling, tissue engineering, microfluidics, drug delivery, etc. have been made possible by the advancement of 3D printing technology. The photopolymerization-based processes used in stereolithography and digital light processing, among other 3D printing technologies, provide users flexibility over the final qualities of the 3D printed materials, including optical, chemical, and mechanical properties [5]. There are several methods for 3D printing that rely on mechanical, electrical, or photochemical methods [e.g. fused deposition modelling (FDM), selective laser sintering (SLS), and stereolithography (SLA)]. There are benefits and drawbacks to each of these 3D printing methods [6]. Engineers, material scientists, and polymer chemists have paid particular attention to photopolymerization-based 3D printing processes as a result of the numerous breakthroughs in polymer chemistry [5]. The photochemical method to 3D printing is among the most alluring since it allows for the fabrication of items through photopolymerization processes involving monomers and oligomers, which has advantages for the environment, the economy, and manufacturing [6].

Photocuring and photocrosslinking are other terms for 3D photopolymerization [5]. The utilization of liquid monomers and oligomers, which are systems that may cure or photopolymerize when exposed to a light source of a certain wavelength in the presence of a photoinitiator system, is the foundation of three-dimensional photopolymerization [7]. To convert photolytic energy into the reactive species that may fuel the chain development through chemical processes, a photoinitiator or photoinitiator system is needed. In most cases, the photochemical process is initiated

by photoinitiators with high molar extinction coefficients at short wavelengths, most frequently UV 400 nm [5]. The two most crucial elements of photopolymers for 3D printing in this method are monomers/oligomers and photoinitiators. In order to create the designed 3D items, photoinitiators absorb the irradiation light from a 3D printer and initiate the photopolymerization processes of monomers and oligomers layer by layer. Monomers and oligomers also determine the final qualities of the produced objects [6].

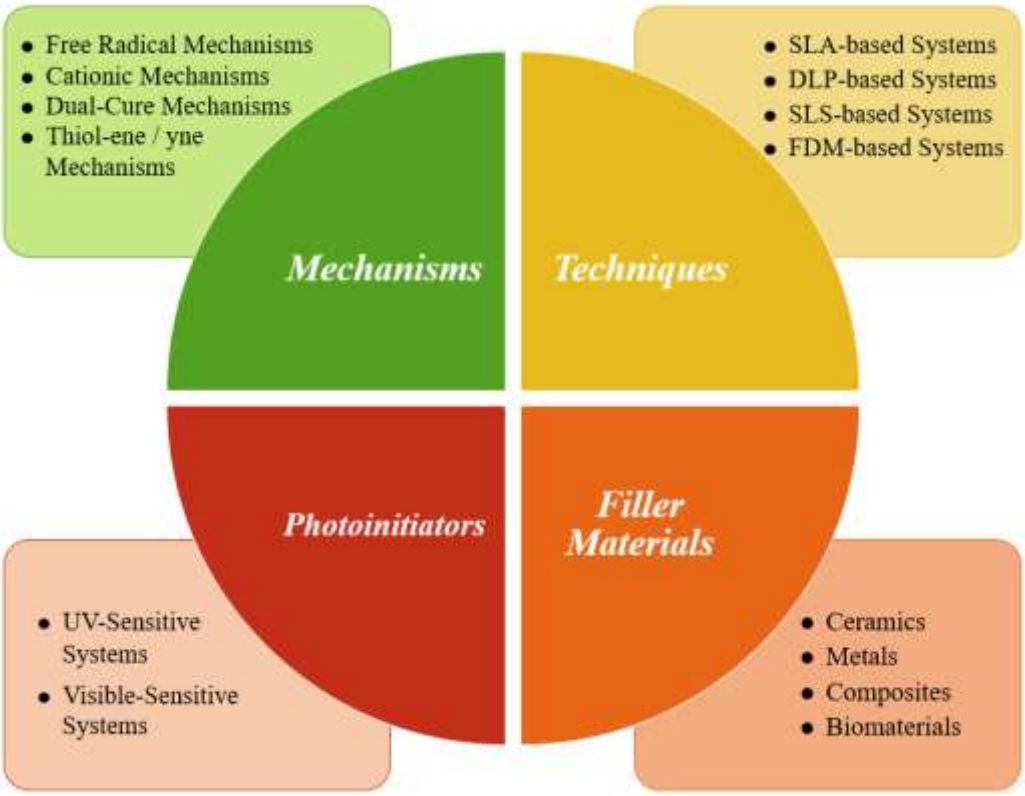

Figure 1.1 : Schematic representation of the main topics covered in 3D photopolymerization.

Considering 3D Photopolymerization from a broad perspective, the points to be considered in this approach process can be divided into 4 main categories. Schematic representation of the main topics covered in 3D photopolymerization is shown in Figure 1.1. In this approach, the mechanism by which the selected monomer/oligomers will proceed and the compatibility of the monomer/oligomers with this mechanism are extremely important. Depending on the types of monomers and oligomers selected, photochemical reaction may vary through free radical mechanism, cationic mechanism, dual cure mechanism or thiolene mechanism. It is vital to select a photoinitiator or photoinitiator system suitable for the selected monomer/oligomer

structure and the mechanism used. There are many commercially available photoinitiator systems suitable for these mechanisms. Techniques based on 3D photopolymerization, including stereolithography (SLA), digital light processing (DLP), fused deposition modeling (FDM), and selective laser sintering (SLS) make it possible to fabricate complex multifunctional material systems in three dimensions with controllable optical, chemical, and mechanical properties [8]. These approaches may also be used to achieve high resolution with low feature sizes. To this purpose, new paths in a variety of industries, including biomedical devices, surgery, dentistry, microfluidics, drug delivery, soft robotics, and tissue engineering, have been made possible by this technology [9].

2. PHOTOPOLYMERIZATION MECHANISMS

Photopolymerization is a technique that cures and thermosets monomers or oligomers in liquid form by exposing them to a light source of a certain wavelength. Photopolymerization is a method that utilizes light energy to convert liquid resin systems into cross-linked solid polymers. It is an efficient, cost-effective, and environmentally friendly approach. Light-curing formulations are typically composed of multifunctional monomers and oligomers with trace quantities of photoinitiators that, when exposed to ultraviolet (UV) rays, generate reactive species. The techniques, photoinitiators, and mechanisms used may differ depending on the characteristics of these monomers or oligomers.

The components of a straightforward photopolymer (resin) system include oligomers, mono- or poly-functional monomers, and a tiny bit of photoinitiator (PI) [10]. The photoinitiating system's backbone is made up of oligomers, which are long chains of molecules, whereas diluting agents are monomers. The photoinitiators are activated when resin is exposed to light, which results in the production of reactive particles, reactive ions, or free radicals. These particles react with monomers and oligomers to generate long chains that lead to photopolymerization [11,12]. Monomers and oligomers cannot generate enough reactive species for polymerization on their own. As a result, only a little amount of PI is required to initiate the process [13]. General presentation of photoinitiated polymerization is shown in Figure 2.1.

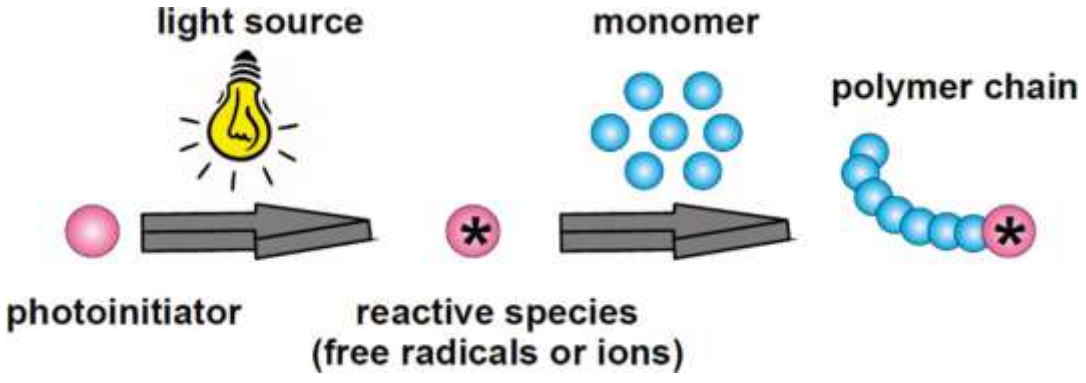

Figure 2.1 : General Presentation of Photoinitiated Polymerization.

More complicated photoinitiating systems, such as co-initiators, inert dyes, photosensitizers, and so on, are being developed to boost photoinitor yield. . Additionally, because resins are highly reactive to radiation, fillers such as ceramic or metal can be added to the base resin formulation to generate a suspension. In these systems, photopolymerized resin acts as a matrix for solid particles. The organic component is subsequently eliminated by a post-processing procedure called debinding. After that, a dense solid component is created by sintering at an optimal temperature from the remaining porous solid structure. A schematic of the material composition for the vat polymerization process can be seen in Figure 2.2. This composition can be either pure resin or advanced components like ceramic or metal suspensions that can be added to the resin before printing [13].

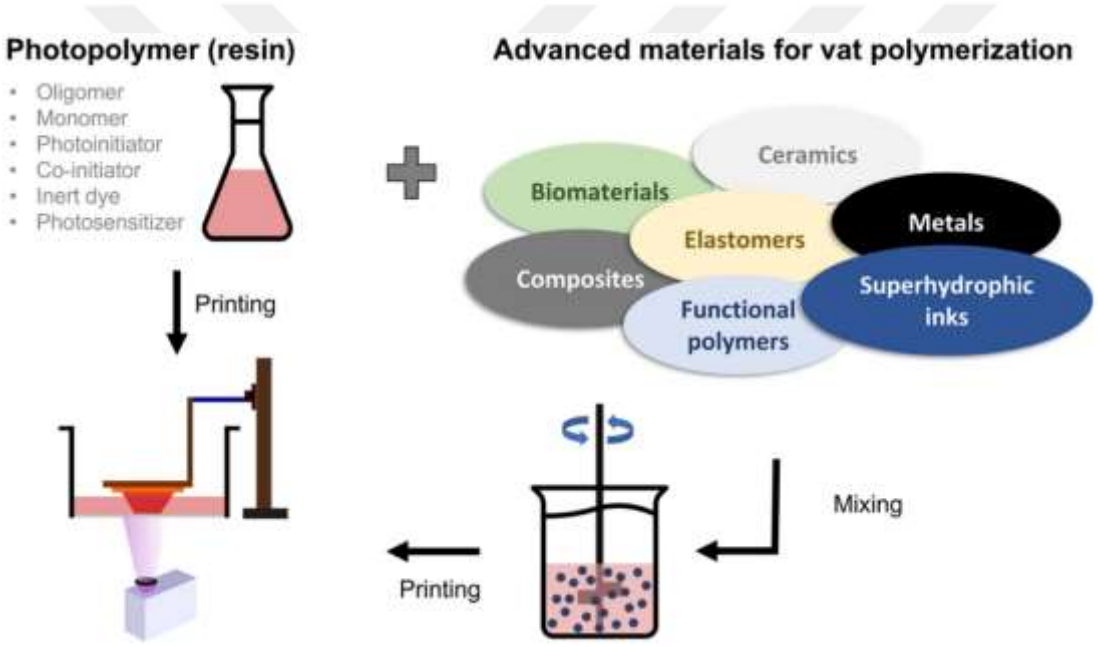

Figure 2.2 : A schematic of the material composition for the vat polymerization process is shown.

The ratio of the components inside photopolymer has a variety of effects on the printing process. Particularly, oligomers with fewer repeating units have a higher molecular weight than monomers. A high oligomer content improves the printed product's mechanical strength but also increases the liquid photopolymer's viscosity, which reduces flowability and hinders the vat recoating process. In contrast, raising the monomer percentage decreases liquid viscosity while increasing the polymerization time to attain comparable mechanical properties. As a result, the ratio of oligomers to monomers is crucial for adjusting the viscosity of the resin, the

exposure period for polymerization, and the final qualities of the printed item [15]. In general, the polymerization stages for all photopolymers when reacting with radiation are the same [13].

2.1 Free Radical Mechanisms

The most common method for commercially polymerizing acrylate and methacrylate oligomers is free radical polymerization using photoinitiators that generate radicals under the action of a UV light source's energy. There are also many radical photoinitiator systems commercially available. Radical generation, initiation, and propagation are widely utilized for fast prototyping since they are relatively quick procedures. The initial stage in crosslinking a photoresin involves light absorption and a photoinitiator or photoinitiator system that transforms photolytic energy into reactive species to promote polymerization [8].

Free radicals initiate UV curing of some monomers, such as acrylate, methacrylate, and maleate/vinyl ether systems. In free radical polymerization, radical formation can occur via two distinct reactions. These are;

• Norrish type I reactions

• Norrish type II reactions.

If we examine the Norrish type I reaction; This reaction takes place by α-cleavage. Upon exposure to UV light, the photoinitiator transforms into a radical couple via homolytic decomposition. These radical pairs directly initiate the polymerization. Absorbed radiation causes bond breakage between a carbonyl group and an adjacent carbon [7].

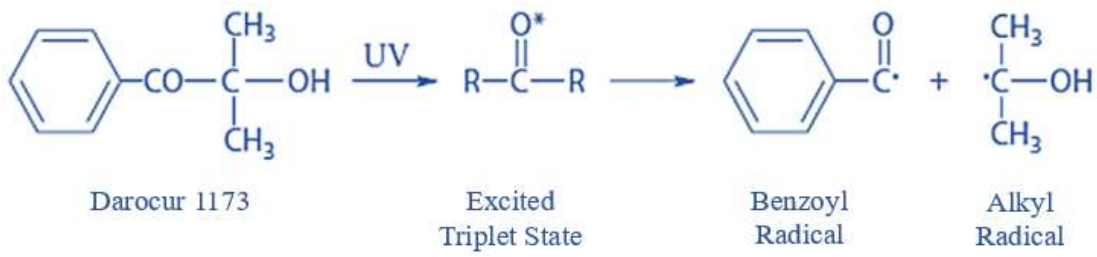

Figure 2.3 : The radical generation reaction of Norrish I type photoinitiators.

Most readily available photoinitiators exhibit the Norrish type I -cleavage reaction and generate radicals when exposed to light. The chemical structures of the photoinitiators

impact the wavelength and intensity of the incident light needed to initiate cleavage [5]. The radical generation reactions of Norrish I type photoinitiators are shown in Figure 2.3.

If we examine the Norrish II type reaction; when light is present in two-component photoinitiating systems, an uncleavable sensitizer and a coinitiator produce excited triplet states [5]. In the Norrish II type reaction, there is a hydrogen scavenging situation. Triplet states of ketones with α-hydrogen react with suitable hydrogen donating compounds, preferably via hydrogen cleavage. The resulting pair of radicals can generate protons in two different ways. The first of these ways; It is the homolytic cleavage of the R-H bond. The second pathway can be generated via proton transfer followed by an intermediate charge transfer complex. The lifetime of excited starters is usually less than 10^{-6} seconds [7]. There are two possible outcomes during this time: either it can radiate light or heat to return to its initial state, or it can create a reactive intermediate that can interact with another free radical or initiate the polymerization of a monomer [18]. The radical generation reactions of Norrish II type photoinitiators are shown in Figure 2.4.

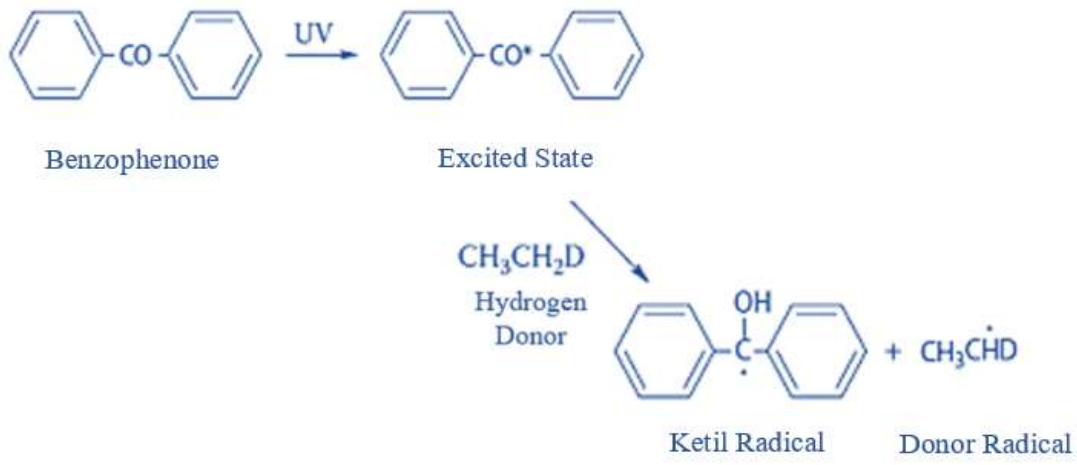

Figure 2.4 : Hydrogen cleavage reaction of Norrish II type photoinitiator.

The most commonly used UV curable systems in free radical polymerization are systems containing acrylate structure. Methacrylates are less preferred than acrylates. This is due to the fact that methacrylates are less reactive. Acrylates, on the other hand, are more harmful than methacrylates. Methacrylates are less irritating to the skin. Acrylate curing typically takes place over vinyl monomers. Therefore, the degree of double bond conversion is the measure of the degree of cure. When acrylate-based

monomers and oligomers are used, oligomers are generally used as binders and monomers as reactive diluents. The most commonly used acrylate and methacrylates are Hexanediol Diacrylate (HDDA), Poly(ethylene glycol) diacrylate (PEGDA), Trimethylolpropane triacrylate (TMPTA), Bisphenol A-glycidyl Methacrylate (Bis-GMA), Bisphenol A Ethoxylate Diacrylate (Bis-EDA), Triethylene Glycol Dimethacrylate (TEGDMA), UDMA, Isobornyl Acrylate. Acrylate and methacrylate structures are given in Figure 2.5 [18].

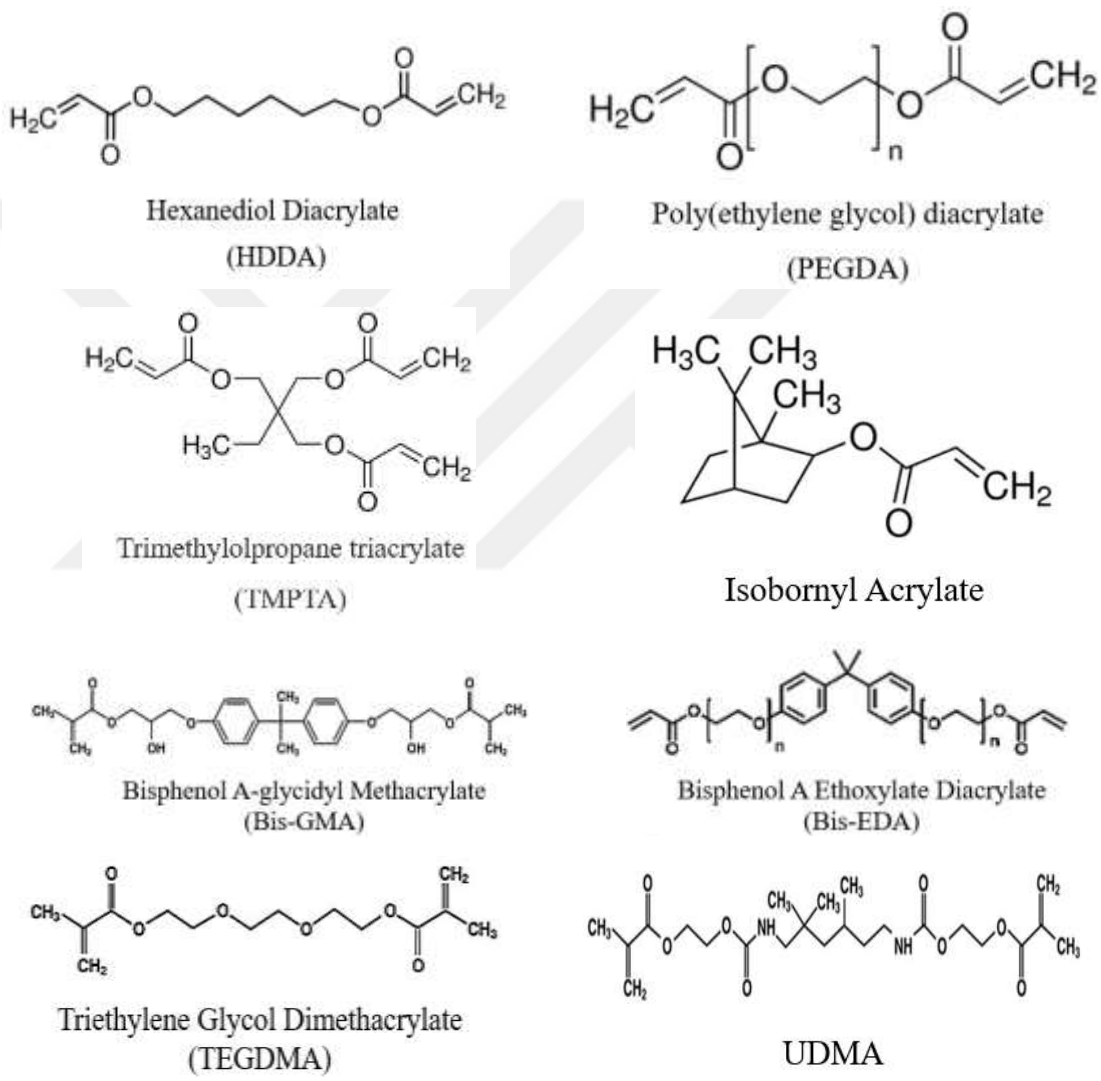

Figure 2.5 : The most commonly used acrylate and methacrylate based curing agents.

Although (meth)acrylate-based resins have proven efficient in 3D photopolymerization, they have several drawbacks. These resins may tend to shrink during the polymerization process. In addition, pure (meth)acrylate resins tend to gel at low conversions, depending on the functionality of the used monomer [23, 24].

Depending on the monomer or oligomer's molecular structure, the degree of shrinkage varies. Cycloaliphatic and aromatic acrylates shrink less than typical monomers like TEGDMA. Bending and deformation can be caused by shrinkage and corresponding stress [26]. Some solutions for reducing shrinking have been suggested. If these discovered techniques should be mentioned, the usage of high molecular weight oligomeric acrylates (with reduced reactive group concentrations) can minimize shrinkage percentage; nevertheless, heating is required to decrease the high viscosity of these resins (during the 3D process) [27]. Another method for reducing shrinkage during photopolymerization is to employ a radical step growth mechanism instead of chain growth polymerization.

The rapid progress of the reaction, the insensitivity of the acrylate structures utilized to pollution during the reaction, their tolerance to a broad variety, and the fact that they may be carried out in a liquid environment are some of the factors that promote the utility of this reaction type. The most important disadvantage of free radical polymerization is that it is oxygen inhibition. Due to oxygen retention, a soft layer forms on the surface after the curing process [14, 15]. In order to prevent this soft and sticky layer, the product prepared for curing should be cut off from contact with oxygen during curing.

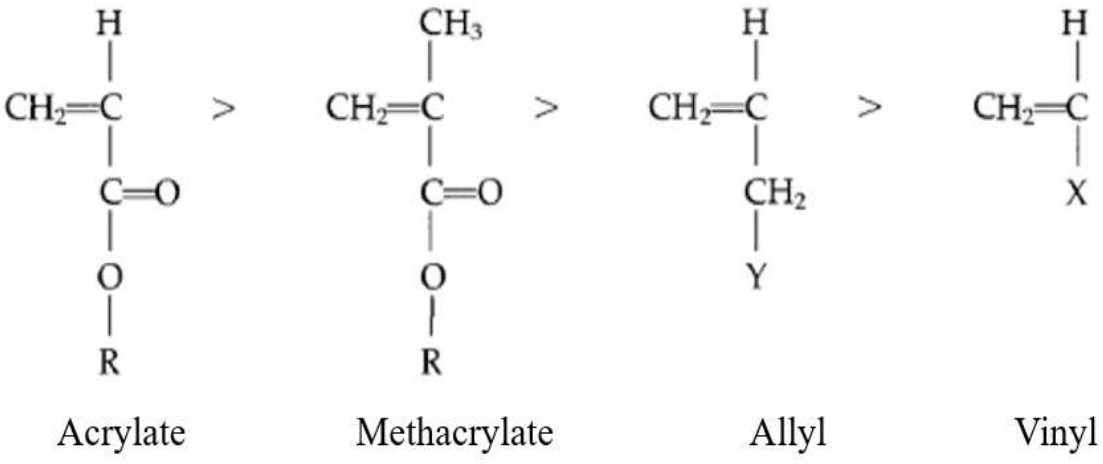

Figure 2.6 : Comparison of curing rates of some chemical groups with UV.

Each monomer used has a varied level of reactivity. Certain monomers polymerize more quickly than others. Vinyl groups, for example, are substantially less UV-curable than acrylates. A comparison of the curing rates of acrylate, methacrylate, allyl and vinyl groups is given in Figure 2.6. R as shown herein may be an alkyl group, Y may be a hydroxyl group, and X may be halogen, phenyl, or alkyl ester [7, 20].

2.2 Cationic Mechanism

The photoinitiated cationic polymerizations have not gotten as much research as photoinitiated free radical polymerizations, despite the fact that they have been known about and studied for a long time [28]. Due to its application to a wide range of formulations based on acrylates, unsaturated polyesters, and polyurethanes as well as the existence of photoinitiators with spectral sensitivity around UV or in the visible region, photoinitiated free radical polymerization has progressed more rapidly [29]. The lack of adequate photoinitiators that can catalyze ionic polymerizations is primarily responsible for the delayed development of cationic polymerization [28].

Ultraviolet energy is used during cationic polymerization to transform the cationic photoinitiator into protonic acid. Protonic acid starts the ring-opening polymerization of epoxy resins and polyethers, in contrast to free radicals, which encourage chain polymerization of acrylate-type monomers.These resins' benefits include their excellent adhesion, resistance to chemicals, and lack of oxygen sensitivity [19]. Improved adhesion resulting from low shrinkage of between 2% and 5% during the photopolymerization step is a significant benefit of cationic systems. The fact that all the products employed are low-viscosity liquids and the chemicals are easily miscible makes these systems simple to control as well. In order to blend the formulation ingredients, a straightforward mixing procedure is typically adequate [20]. Examples of monomers used in cationic 3D photopolymerization is shown in Figure 2.7.

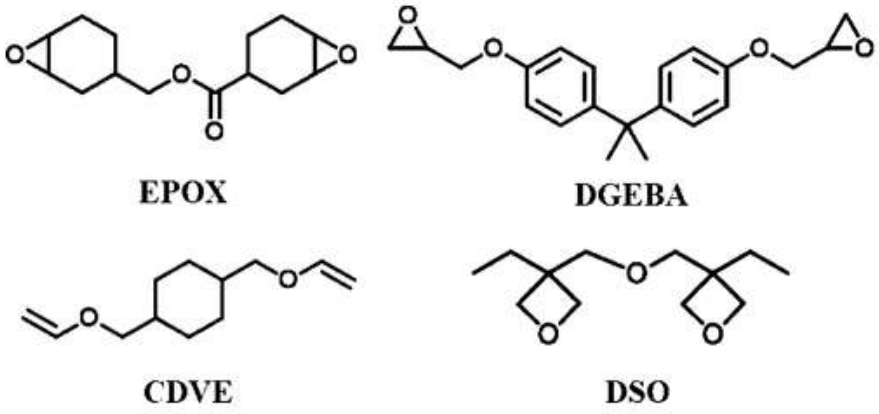

Figure 2.7 : Examples of monomers used in cationic 3D photopolymerization.

Additionally, oxygen inhibition has no influence on cationic polymerization. Volatile emissions, high viscosity, molecular oxygen inhibition limitations, and toxicity problems are all eliminated via cationic photopolymerization. Epoxides and vinyl

ethers are the most often used monomers in cationically polymerized systems [32, 33]. Several of the most common applications for cationic polymerization are surface coatings, printing plates, and photoresists [34].

These systems have been employed in 3D applications as well as in other industries, using epoxy monomers that are widely accessible, such as bisphenol A diglycidyl ether (DGEBA) and 3,4 epoxycyclohexanemethyl 3,4 epoxycyclohexylcarboxylate (EPOX). The reactivity of the monomers varies depending on their molecular structure; for instance, cycloaliphatic epoxide-containing monomers exhibit substantial double ring strain and rapidly polymerize [35]. Additionally, SLA-based systems have made considerable utilization of cationic polymerizable vinyl ether monomers such 1,4-cyclohexane dimethanol divinyl ether (CDVE). For instance, CDVE and epoxides can be used to enable faster polymerization [36]. Additionally, disubstituted oxetane (DSO) monomers, which exhibit strong reactivity (relative to epoxides) with comparable low shrinkage rate and increased water resistance, can be employed in cationic photopolymerization [37, 38]. Epoxide monomers are highly sought-after due of the low volumetric shrinkage (3%) that occurs during ring-opening photopolymerization [39].

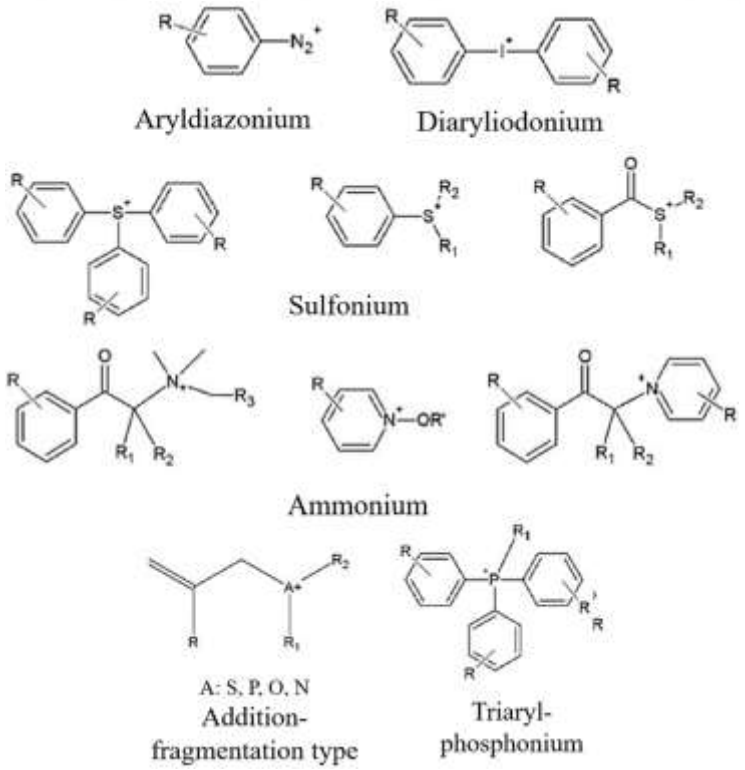

Figure 2.8 : Some often use onium salt photoinitiators.

Research on cationic polymerization gained more attention in the late 1970s because to the development of onium salts appropriate for the initiator function in cationic polymerization. Furthermore, significant advancements have been achieved, particularly in the synthesis of photoinitiators for cationic polymerization [28]. The most commonly photoinitiators used in cationic polymerization are iodonium and sulfonium salts [40-42]. Some often use onium salts were as given below (Figure 2.8).

The utilization of onium salts, pyridinium salts, latent sulfonic acids, and iron arene complexes, which are thermally stable yet photochemically active, has significantly advanced the field of cationic polymerization. Direct and indirect acting systems can be thought of in relation to onium salts, which are the most well-known cationic photoinitiators [29].

2.2.1 Direct initiation

The photoinitiator decomposes in the cationic photopolymerization technique, in which the polymerization process begins directly, by absorbing the light at the suitable wavelength. Then, the cationically polymerizable monomer reacts with the reactive species radical cation and protonic acid to generate these active species, which then cause the polymer chain to begin to propagate. (Figure 2.9) [43]. The photoinitiator molecules often used in this process are those that absorb light at wavelengths in the UVA, UVB, and UVC areas of the electromagnetic spectrum [44]. The fact that the anions in onium salts employed in cationic polymerization are non-nucleophilic and have no negative effects on the polymerization process is one of their most advantageous features.

One of the most beneficial properties of onium salts used in cationic polymerization is that the anions they contain are non-nucleophilic and do not have a negative effect on the course of the polymerization. if these anions were not non-nucleophilic, they could suppress the propagation of polymer chains. If these anions were not non-nucleophilic, they could suppress the propagation of polymer chains [45].

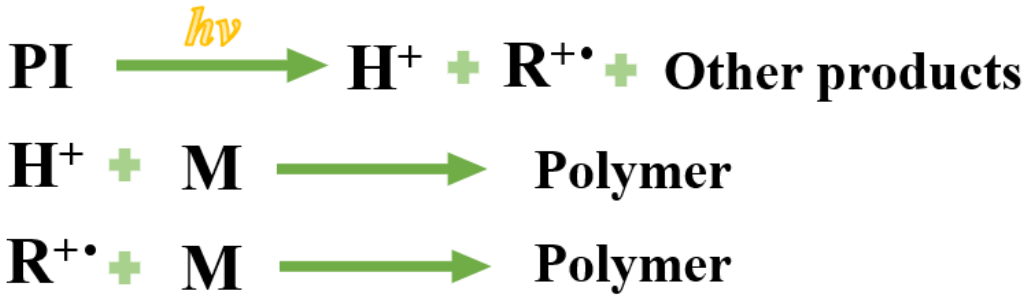

Figure 2.9 : Direct initiation in photoinduced cationic polymerization.

2.2.2 Indirect initiation

In photopolymerization procedures, incident light at the wavelength that the initiating molecules absorb initiates the chemical reactions. Therefore, the initiator molecule determines the appropriate light wavelength to utilize. The capacity to absorb in the UV wavelength, which requires relatively more energy, is present in the majority of initiator molecules. Complexes are formed utilizing some electron-rich compounds in addition to the initiator molecules to get around this issue. By using these various methods, it is possible to make the wavelength of the light being used higher than the wavelength at which the photoinitiator absorbs [46].

2.3 Dual-cure Mechanism

Dual-curing resin systems combine two distinct polymerization processes, either simultaneously or sequentially. These dual cure formulations create interpenetrating polymer networks (IPNs) to regulate the photopolymerization rate and crosslink density, hence regulating characteristics appropriate for various applications [5]. A unique type of polymer blends called interpenetrating polymer networks is one in which both polymers are typically in network form [48, 49]. Comparable to the sum of its constituent components, the resultant interpenetrating polymer network (IPN) possesses excellent qualities [50]. These polymerization processes can be activated by stimuli that are comparable or distinct, such as a combination of UV and temperature or a combination of two different temperatures. Many dual-curing resin systems that combine a UV curing component and a thermal curing composition have been produced and brought to market over the past 20 years [51].

IPNs' main benefit is that they combine the qualities of the two different types of polymer networks. Structures formed by combining the properties of two different

polymer network types can exhibit superior properties. The photoinitiated polymerization of a monomer mixture is a most simple method of producing IPNs. Epoxides and acrylates, in particular, which polymerize by a cationic mechanism and a radical mechanism, respectively, are two types of monomers frequently utilized in UV radiation curing. Combining these two types of monomers makes it simple to synthesize IPNs [52]. This resin, which was produced by synthesizing acrylate and epoxy monomers, is utilized to get over the drawbacks of acrylates and epoxides. Because the monomers can polymerize in this situation by a variety of methods and the final products combine the qualities of both acrylates and epoxides, they are appropriate for a variety of applications [53]. Epoxy-acrylates are characterized by thermal resistance, hardness, non-yellowing and flexibility. In this instance, the ether and carbon-carbon linkages enhance chemical resistance while the epoxy backbone promotes strength and flexibility during curing [7].

Epoxides and acrylates go through distinct polymerization processes and do not significantly react with one another. Therefore, the final polymer is not a copolymer, instead it is an interpenetrating network (IPN). These systems have the advantage of having significantly lower sensitivity to oxygen inhibition [8].

These applications benefit from the rapid UV cure, which lowers initial processing times to a few seconds or less, while thermal curing methods offer the proper final mechanical characteristics. The thermal curing composition of these resin systems consists of a resin with certain final properties, such as epoxy or polyurethane, and a suitable curing agent. The UV component of these resin systems typically includes an acrylate monomer, acrylate oligomer, and photoinitiator [51].

An interpenetrating polymer network (IPN) is rapidly produced during the initial UV curing, along with a weak intermediate structure [56, 57]. In a subsequent, thermally activated stage, this intermediate structure is completely cured, creating the ultimate monolithic characteristics necessary for the application [51].

By adjusting the formulation's composition as well as the cure's duration and temperature, it is simple to control the extent of both curing reactions and the qualities of the intermediate material in dual-curing processes [58]. The intermediate material in a sequential dual-curing process will have stable characteristics and won't cure unless the second reaction is started. There are some important conditions for

successful sequential dual-curing. First of all, both polymerization reactions must be selective and compatible. This ensures that undesirable inhibition or reactivity effects do not occur. In addition, the substances used must have different reaction rates. Because they can be triggered using different stimuli such as UV light or temperature. They also need to have sufficiently different reaction rates to be controlled from a kinetic point of view in terms of time and temperature. The ability to modify the final and intermediate stage characteristics, which is crucial for their usage in advanced applications, is a significant benefit of sequential dual-curing [50]. For instance, in systems including DGEBA and ECC, the epoxy component undergoes considerable "dark cure," continuing to polymerize after the light is turned off, whereas the acrylate component responds considerably more quickly [52]. The chemical structures of Bisphenol A diglycidyl ether (DGEBA) and 3,4-Epoxycyclohexylmethyl 3,4-epoxycyclohexanecarboxylate (ECC) are shown in Figure 2.10.

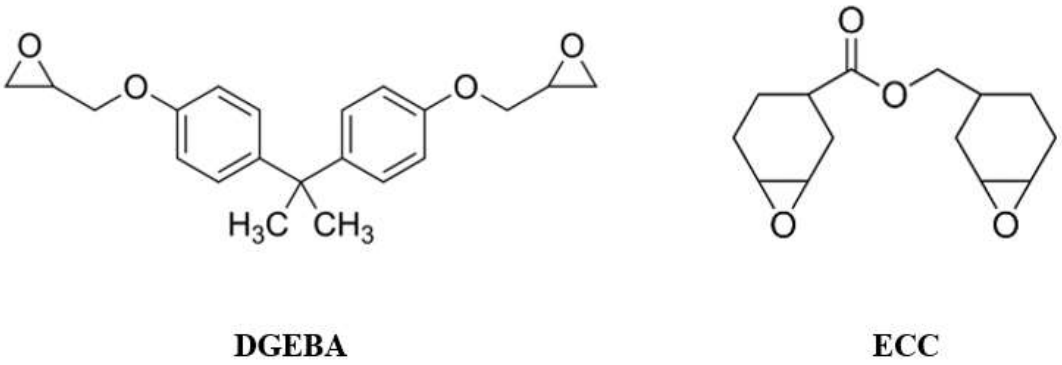

Figure 2.10 : Bisphenol A diglycidyl ether (DGEBA) and 3,4-Epoxycyclohexylmethyl 3,4- epoxycyclohexanecarboxylate (ECC).

Dual-curing systems may also be used to describe hybrid organic-inorganic materials made through the use of curing and the sol-gel method [59, 60]. In addition, there is a hybrid monomer called 3,4-epoxy-cyclohexylmethyl methacrylate, which has both epoxide and methacrylate groups. So both cationic and free radical compounds can photopolymerize. Therefore, it can be employed in this system and the incompatibility of two distinct kinds of monomers is eliminated [61]. Moreover, the idea of dual-curing transcends such notions and enables the creation of specially customized materials with processing flexibility that are beneficial for a variety of cutting-edge, high-value applications [50].

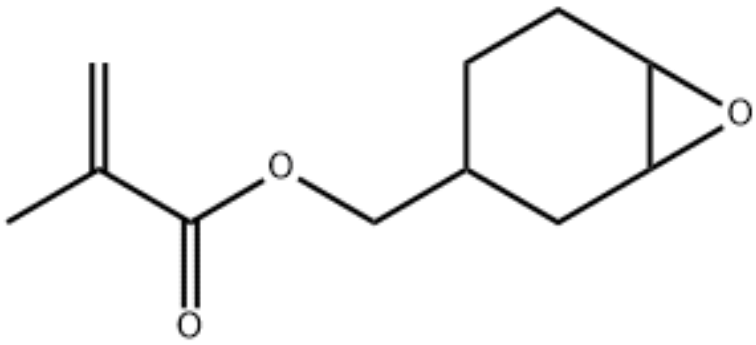

Figure 2.11 : 3,4-Epoxycyclohexylmethyl methacrylate.

The field of 3D printing is where one can find another fascinating use for dual-curing systems. Due to the decrease in shape distortion and the additional postcure after building, hybrid dual-cure formulations combining cationic polymerization of epoxides and radical homopolymerization of acrylates are recognized to significantly improve the quality of printed parts and are in fact frequently used in 3D printing applications. The variety of potential polymerization reaction combinations, the ability to control the material structure, and the extent of reaction following 3D printing, however, make the use of dual-curing systems in this field considerably more expansive, particularly for sequential systems [62]. In addition, they are employed in various sectors of the industry due to their superior chemical, low cost, corrosion resistance, favorable mechanical qualities, and excellent processability [63]. The main drawbacks of these materials are their high viscosity and poor external durability [7]. The chemical structures of 3,4-Epoxycyclohexylmethyl methacrylate.is shown in Figure 2.11.

The use of epoxy acrylate prepolymers has increased tremendously in recent years. They can be used as lithographic paints, varnishes, or wood coatings. Additionally, vacuum metalizing base coatings, and adhesive laminates are prominent uses for them [19 -23].

2.4 Thiol–Ene and Thiol–Yne Systems

The photopolymerization of thiol-ene and thiol-in proceeds exhibiting a uniform cross-linked network compared to the (meth)acrylate-based photopolymerization process. Thiol-yne networks exhibit greater crosslink density, glass transition temperature, and modulus than thiol-ene networks due to the second addition with thiols [70]. In reactions where Thiol–Ene and Thiol–Yne Systems are used, two different ways can

be followed for polymerization to occur. These pathways are Michael addition reactions or radical step-growth polymerization [24, 66]. There are several reasons why thiol-ene-based photocurable resins are preferred over (meth)acrylate-based formulations. Low oxygen inhibition is one of the most significant advantages of the Thiol-Ene and Thiol-Yne Systems. Thiols react as strong hydrogen donors to a created peroxide radical, forming a reactive thiyl radical and so reducing oxygen inhibition [67].

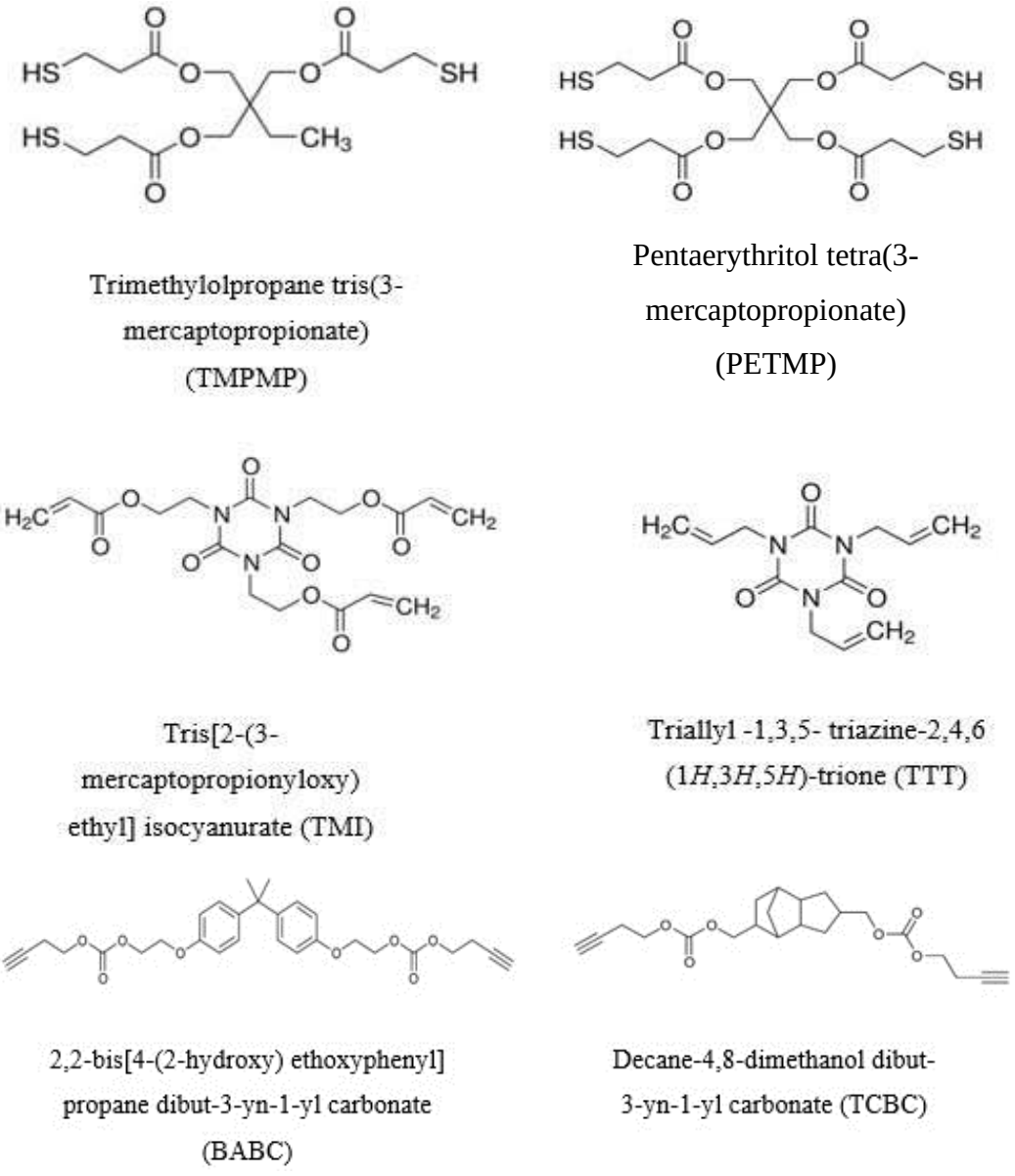

Figure 2.12 : Commonly used monomers in Thiol–Ene and Thiol–Yne Systems.

Acrylate based resins have higher shrinkage stress than thiol-ene based resins. The difference in the amount of shrinkage stress between these two systems is due to the formation of a relatively high conversion gel point resulting from the step-growth

mechanism of the thiol-ene systems [68]. The third and last major advantage of thiol-ene systems over other systems is the high level of biocompatibility. Thiol-ene systems are more biocompatible than (meth)acrylate-based networks [69]. Thiol-ene chemistry has developed into a desirable method for producing a variety of 3D structures, such as hydrogel constructions, optical wave guides, and woodpile photonic crystals, as a result of these properties.

Thiol-ene based systems have advantages as well as disadvantages. However, there are few problems that prevent their further development in 3D applications. Poor shelf life and bad odor are examples of these issues. Thiol-ene based systems have a short shelf life due to the formation of oxidative disulfide bonds [5].Commonly used monomers in Thiol–Ene and Thiol–Yne Systems are shown in Figure 2.12

2.5 Photoinitiators

Photoinitiators were rapidly developed by businesses such as BASF, AKZOCIBA GEIGY, and others between 1960 and 1970. When exposed to ultraviolet light, photoinitiators turn light energy into chemical energy by producing free radicals or cations. By UV reaction, they can be divided into two or more particles, at least one of which will interact with oligomers or monomers to bind them together [71]. The capacity of the photoinitiator to respond to the wavelength of the light source employed, as well as the initiator's absorbance ability to match the kind of light source (UV or visible light), is crucial for the overall efficiency of the process [30]. These can be found naturally or chemically synthesized, and they are sensitive to certain wavelengths of light. Photoinitiators are a small part of photopolymers.

The majority of monomers or oligomers do not produce reactive species on their own to initiate photopolymerization. As a consequence, organic photoinitiators of low molecular weight are utilized in resins to produce reactive species by attacking the functional groups of monomers or oligomers. Free radical photoinitiators generate free radicals that rapidly attack the double bonds of certain monomers such as methacrylates and acrylates following absorption of incoming UV light. Unlike free radical photoinitiators, cationic photoinitiators produce acids when exposed to light. When exposed to light, cationic photoinitiators, as opposed to free radical photoinitiators generate acids. The resulting acids easily react with certain monomers, such as epoxides and vinyl ethers, to initiate polymerization [72]. The type and

concentration of photoinitiators, as well as the fundamental kinetic parameters of the monomer, all influence polymerization [29].

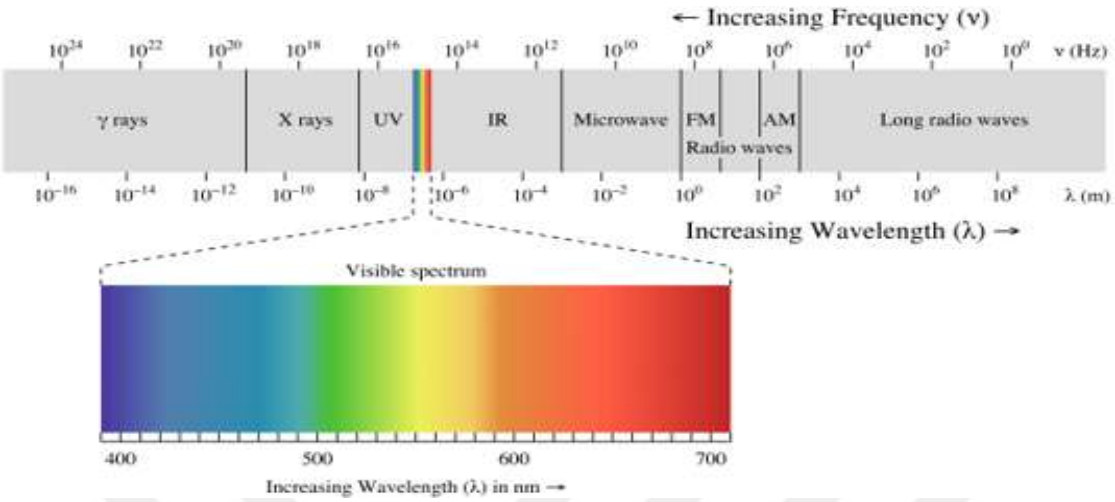

Figure 2.13 : Electromagnetic spectrum.

The reaction is initiated by light irradiation, and a photoinitiator system or photoinitiator is in charge of converting photolytic energy into reactive species. The light source might be xenon lamps, LEDs, lasers or mercury arc lamps. The photon source's wavelengths can range from 190 nm to 400 nm for UV light, from 400 nm to 700 nm for visible light and from 700 nm to 1000 nm for infrared radiation. Electromagnetic spectrum is shown in Figure 2.13.

The reactions that need to be known in order to adequately understand the ultraviolet light curing technology are photochemical reactions. Therefore, the Jablonski diagram is of great importance. The Jablonski diagram describes the transitions that occur in photochemical reactions. The Jablonski diagram shown in Figure 2.14 is a diagram that schematically represents energy levels and molecular transition energies [17].

The ground state in the Jablonski diagram is called S0. The electronically excited first, second, and nth singlet states are shown as S1, S2, and Sn, respectively. The triplet states are similarly designated as T1, T2, and Tn. If all the electrons of an excited atom are paired and their spins are opposite, this arrangement is called a singlet state. The arrangement in which two unpaired electrons have parallel spins is also called the triplet state. As shown in the Jablonski diagram, there are three different deactivation pathways in which an excited molecule returns to its ground state. The first of these three different deactivation ways; The molecule can return to the ground state directly. This process is followed by the fluorescence, which is the emission of light with

various wavelengths. In other words, if a photon emission occurs while the process of returning to the ground state is taking place, this process is called fluorescence. The second of these three different deactivation ways; The process from the triplet to the ground state is accompanied by phosphorescence emission. That is, the emission of a photon from the triplet state is called phosphorescence. The last one of the deactivation ways is; The molecule can use the excitation energy to enter a chemical reaction.

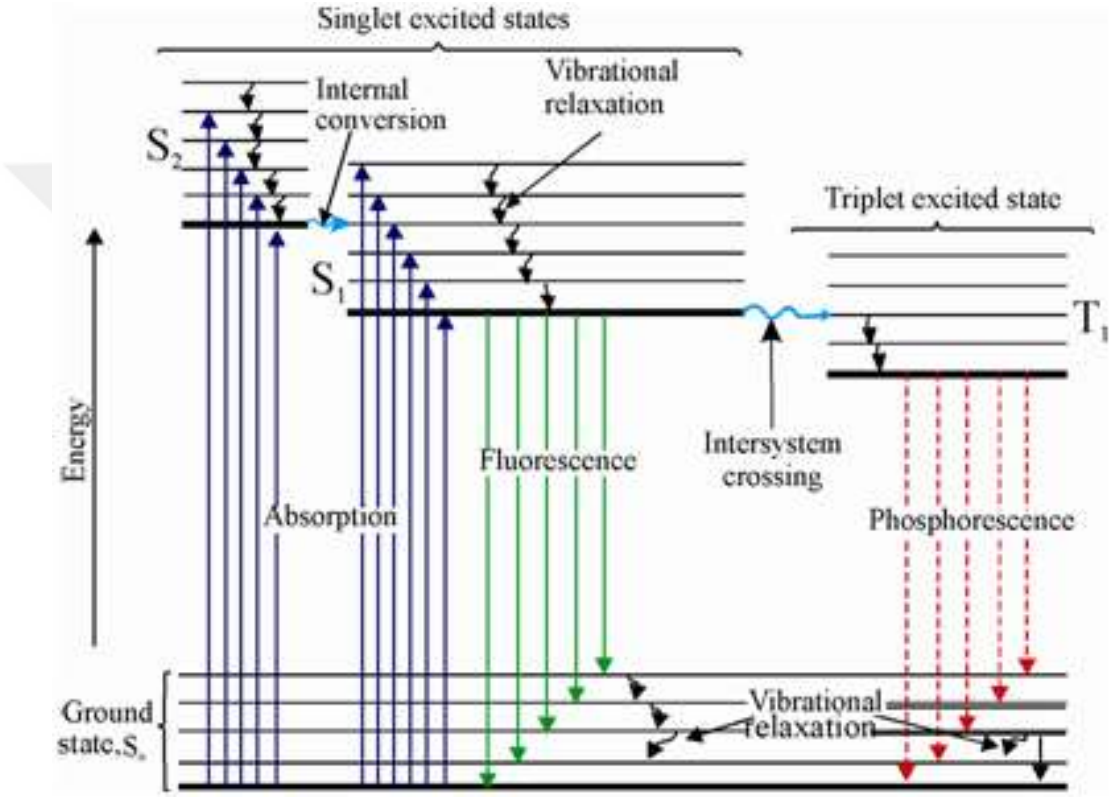

Figure 2.14 : Jablonski diagram.

The Jablonski diagram is important; because the absorption of UV energy by a photoinitiator causes the energy changes shown in the Jablonski diagram to occur. First, a higher energy singlet state is formed, and then a transition between systems to a lower energy but more stable triplet state occurs. Most photoinitiators generate radicals in the triplet state; however, some can also interact as excited singlets. For free radicals to form, a photoinitiator must absorb as much UV energy as possible and become excited. A photoinitiator also demonstrates one or more absorption peaks at different wavelengths where the conversion of UV energy will be most effective [15,29].

2.5.1 UV light-sensitive photoinitiator

A variety of UV light sensitive photoinitiators that are commercially available have been employed in 3D applications. In general, the Irgacure family of photoinitiators is widely used. UV radiation exposure can cause a variety of eye diseases. Commonly used UV light sensitive photoinitiators are given in table 2.1.

Table 2.1 : Commonly used UV light sensitive photoinitiators.

Compound	Chemical Structure	Light Absorption (λ_{max})
Irgacure 184	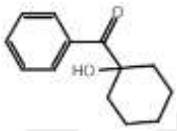	246 nm, 280 nm, 333 nm
Phenyl bis phosphine oxide (BAPO, Irgacure 819)	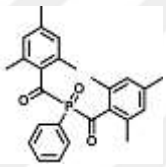	295 nm, 370 nm
2-Hydroxy-2-methyl-1-phenyl-propan-1 (Irgacure 1173)	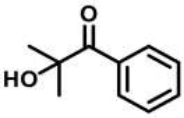	245nm, 280nm, 331 nm
2,2-dimethoxy-2-phenylacetopenone (Irgacure 651 ya da DMPA)	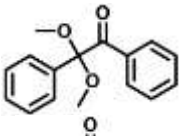	252 nm, 340 nm
Benzophenone	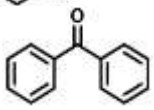	253 nm
2-Hydroxy-4'-(2-hydroxyethoxy)-2-methylpropiophenone (Irgacure 2959)	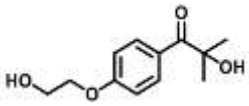	274 nm

2.5.2 Visible light-sensitive photoinitiators

Visible light can overcome the restrictions of high-energy UV light exposure and lower the dangers of eye injury. In comparison to UV light, visible LEDs are more ecologically friendly, have a lower thermal effect, and have a longer lifetime while emitting no ozone. Also, longer wavelength lights are also safer to utilize on live cells. As a result, visible light photoinitiators are commonly used in dentistry and biomedical

applications. Due of these advantages, the use of visible light in 3D applications has evolved through the use of photoinitiators that are sensitive to visible light. Commonly used UV light sensitive photoinitiators are given in table 2.2 [5].

Table 2.2 : Commonly used Visible light sensitive photoinitiators.

Compound	Chemical Structure	Light Absorption (λ_{max})
Camphorquinone (CQ)	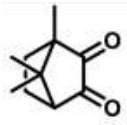	468 nm
Trsi (2,2-biphridyl) dichlororuthenium(II) hexahydrate (Ru)	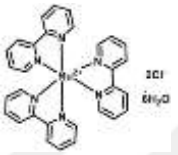	453 nm
Ivocerin	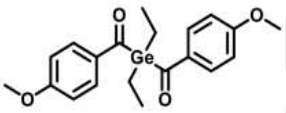	408 nm
Eosin Y	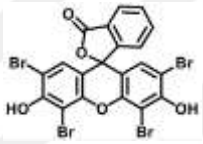	524 nm
Zinc tetraphenylporphyrin (ZnTPP)		420 nm

3. ADDITIVE MANUFACTURING (AM)

The 3D Systems Corporation developed the first 3D printer in 1984. Sterolithgraphy Apparatus was the name given to it. Unfortunately, 3D printing technology was prohibitively expensive and did not benefit any industry until the 2000s. However, The cost of 3D printers, drastically decreased in the twenty-first century, enabling them to be used in a wide range of sectors [75].

Three-dimensional (3D) printing, also known as additive manufacturing (AM), has recently gained attention as an environmentally friendly technique that promotes efficient production while consuming less energy and material [76]. Small amounts of material are processed all at once in additive manufacturing, which is a method that involves adding to one another in order to generate the required component straight from a CAD model [12]. Rapid prototyping, layered manufacturing, direct digital manufacturing, and additive fabrication are only a few of the technologies included in the concept of additive manufacturing, which also includes 3D printing [75]. The manufacturing process of additive manufacturing is shown step by step in Figure 3.1.

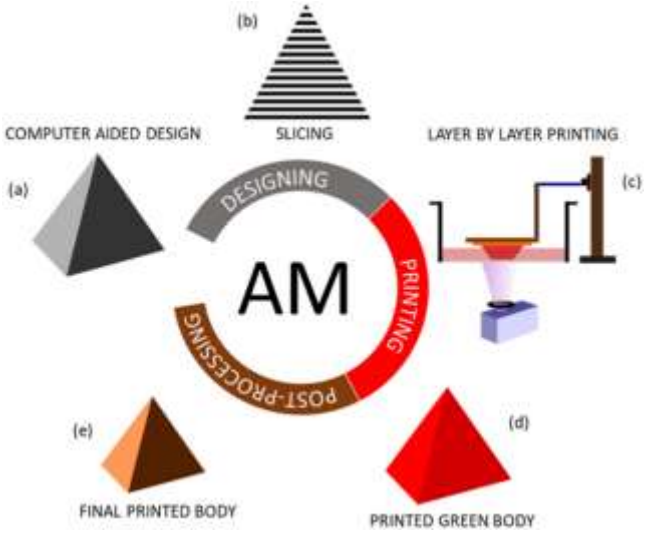

Figure 3.1 : Manufacturing procedure in AM that is step-by-step. The CAD modeling (a) and 3D object slicing process (b) constitute the design phase. In the printing process, these sliced pieces layers are printed one after the other (c).The printed green body (d) is then put through post-processing to become the final printed body(e).

AM is essentially the process of combining materials to produce objects from 3D model data, often layer by layer. A wide range of materials, including polymers, resins, metals, ceramics, glass, rubbers, and concretes, can be employed. However, although having a similar description, 3D printing also refers to a process that combines AM with sterolithography, fused deposition modeling, and selective laser sintering [75]. A wide range of important sectors, including aerospace, automotive, consumer goods, dentistry, and medical items, have the potential to be influenced by additive manufacturing technology [12].

The ability of 3D printing literally lies in the fact that it allows for numerous material innovations during the production process and significantly reduces the time between tool changes on a larger scaled manufacturing line, while maintaining a higher level of customization in the resulting mass manufacturing. Due to the lack of technological constraints imposed by conventional manufacturing methods, 3D printing has the significant advantage of making it easier to construct complicated free form geometries.

There are 18 distinct kinds of 3D printing techniques. These categories can be distinguished depending on the physical properties of the printed material, as well as the method utilized to fuse the material at the molecular level (thermal, electron beam, laser or ultraviolet light). Selective Laser Sintering (SLS), Fused Deposition Modeling (FDM), Selective Laser Melting (SLM), Powder Bed Fusion, Electron Beam Melting (EBM), and Stereolithography are the most widely utilized techniques. Currently, it is possible to print polymers, aluminum, steel, titanium alloys as well as ceramic composites with minimum layer thicknesses of 20 - 100 μm, depending on the method and the physical state of the material.

Given that costs have surely fallen as a result of the significant advancements in technology over the past ten years, 3D printing offers a novel method for producing some complex, low-volume items that is both cost-effective and simplifies the management of resources. Many companies have recently embraced additive manufacturing technology and are beginning to reap the benefits of their investment. The technology is evolving and is making its way into several sectors [75].

3.1 Stereolithography

Stereolithography (SLA) is the most widely used and researched rapid prototyping method. For polymeric materials, stereolithography is regarded as one of the best additive manufacturing processes in terms of geometrical and dimensional accuracy. Many investigations conducted in recent years have revealed that the production of ceramic resins, using a specific blend of monomeric components and ceramic powders, enables the development of complicated form geometries through the photopolymerization process [79]. 3D Systems invented stereolithography in 1986, and it is the origin of all additive manufacturing Technologies [4]. Nowadays, stereolithography along with FDM and SLS, is one of the three primary technologies used in 3D printing. The stereolithograph apparatus (SLA) equipment in this technique turns liquid polymers into solid products using a UV laser [71]. The energy necessary to initiate the photopolymerization process, bond many small monomers, and produce a highly cross-linked polymer is supplied by the laser beam [80].

Stereolithography works by hardening the liquid photopolymer on the surface of a filled vat with a UV beam or laser. Because practically every technology requires 3D design (such as CAD), which is a digital representation of an item, the main principle of operation in all 3D printers is similar. The drawn file must then be converted into another printer-readable system known as Standard Tessellation language to printer-readable form. The addition of layers on top of a liquid is accomplished using a laser beam that is controlled by a computer system [71].

A series of chain reactions are initiated in this technique by beaming UV light (or electron beams) onto a resin layer or a monomer solution. The monomers utilized (often epoxy- or acrylic-based) change into radical forms and become active when exposed to UV radiation. These active monomers are rapidly transformed into polymers [81, 82]. Liquid photopolymers are used as a raw material in SLA. When liquid photopolymer is dropped onto a perforated platform, the UV laser hits the platform and shapes the printed product. In other words, laser beams sketch each layer of the item being printed and solidify the photopolymers [71]. When printing is finished, the residual component is removed from the media utilizing various post-operative techniques [12].

The most significant benefit of SLA is the product scale, which implies that the more costly the 3D printer, the higher quality product manufactured. The main downside of this technique, on the other hand, is that printing takes a long time [75]. The resins previously used in stereolithography techniques were low molecular weight polymers such as epoxy macromers or polyacrylate. Due to their higher temperature resistance, decreased moisture absorption, and reduced shrinkage compared to previously available acrylate-based materials, epoxy-based and hybrid polymers are now preferred over acrylates [71]. Stereolithography process is shown in Figure 3.2.

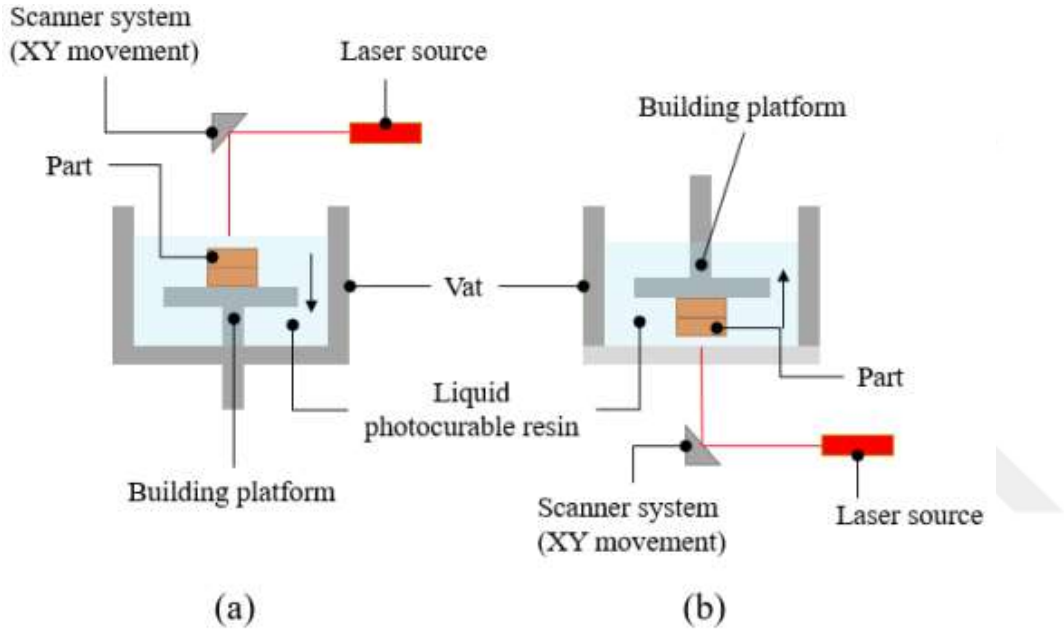

Figure 3.2 : Stereolithography process: (a) top-down and (b) bottom-up apparatus.

3.2 Digital Light Processing

Digital light processing (DLP) is a new technology and apparatus that enables rapid printing while maintaining excellent fabrication precision [85]. By using a projected light source to cure a full layer at once, DLP is an AM technique used to print photopolymer objects [13]. As with stereolithography, this approach employs a photopolymer. Unlike the stereolithography apparatus technique, which employs a point laser as a light source, the Digital light processing technique uses a digital projector as a light source, resulting in reduced drastically printing time [86]. DLP was first developed for pure resins, but subsequent improvements have shown its potential in the polymerization of ceramic and metal-loaded solutions, allowing the manufacture of ceramic and metal components following appropriate debinding and sintering [13].

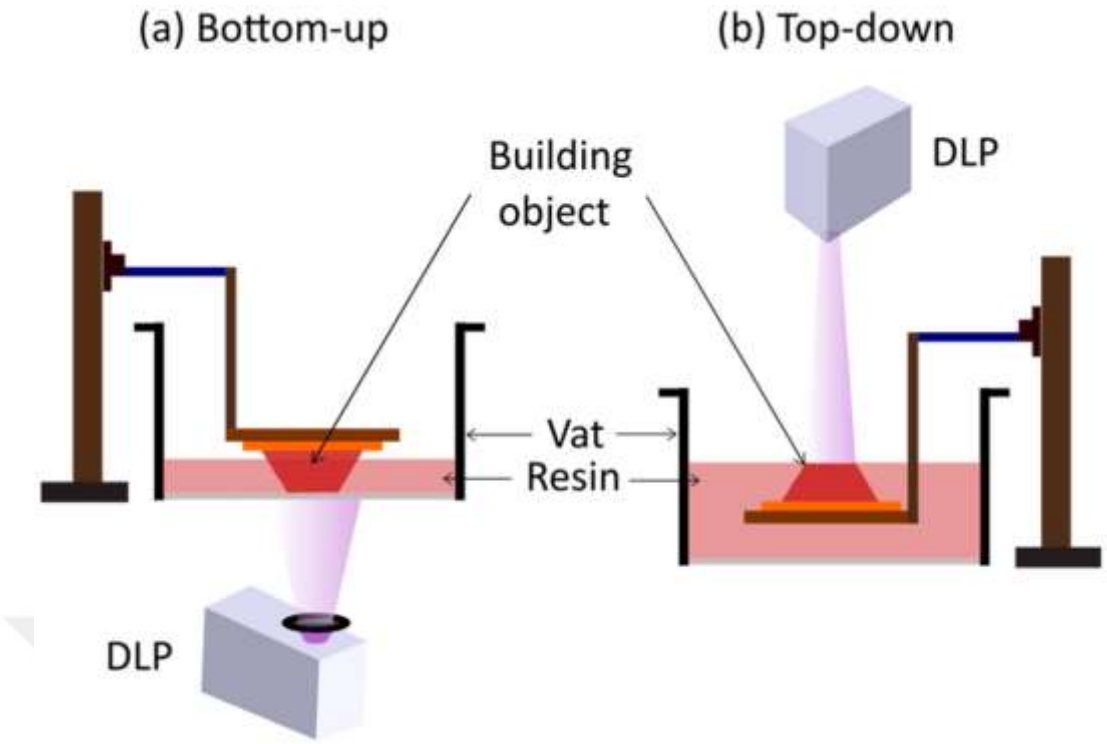

Figure 3.3 : The printing process based on DLP employs two distinct geometries. a Bottom-up: By polymerizing the layers that are visible from the vat's bottom. b Top-down: By polymerizing the layers that are visible from the top of the vat.

In theory, the printing process is the same for all DLP-based printers. Geometric configurations, on the other hand, may differ. DLP typically employs two geometric configurations: bottom-up and top-down. These bottom-up and top-down configurations are shown in Figure 3.3. The build head is submerged in the vat in the Bottom-up configuration depicted in Figure 3.3a; the immersion height is equal to the desired layer thickness. UV light may pass through the vat's transparent bottom and project the picture onto the thin layer of liquid resin that is sandwiched between the build head and the base of the vat. The DLP source is located on top of the vat in the top-down design (Figure 3.3b), in contrast, and the build head is completely submerged inside the vat. The build head's depth is maintained at the selected layer thickness. The DLP source situated above the vat cures the thin layer above the build head [13]. The creation of complex objects such as electrically conductive constructs, organic inorganic hybrid networks, highly stretchable photopolymers, engineered nerve guidance conduits, reprocessable thermosets, and luminescent 3D structures has all been accomplished using DLP-based printing [5].

3.3 Fused Deposition Modelling

Fused Deposition Modelling (FDM) was initially commercialized by Stratasys in 1991, with patents given to the company's founder, Scott Crump, in 1992 [87]. Fused Deposition Modelling is defined as a nozzle-based technology that incorporates additive manufacturing techniques [88]. The FDM technique is based on layer-by-layer fusing and solidification of the thermoplastic polymer after it has been heated to semi-solidity. FDM is suitable for engineering models, conceptual designs, and prototypes for functional testing where temperature, precision, exposure to chemicals, and mechanical strain are key variables [4].

Establishing optimization parameters is crucial for proper manufacturing procedures before the process begins. The parameters mentioned include printing speed, plate, nozzle diameter and filament diameter, nozzle temperatures and layer thickness based on material characteristics [88]. Some of these benefits are the method's speed, low cost, and ease of operation. The process's simplicity makes it suited for the creation of a wide range of thermoplastic polymers, which may offer up potential for Rapid Manufacturing. Figure 3.4 shows a model of the FDM method, which may produce components from polycarbonate, polyphenyl sulfone, and acrylonitrate butadiene styrene (ABS) [87].

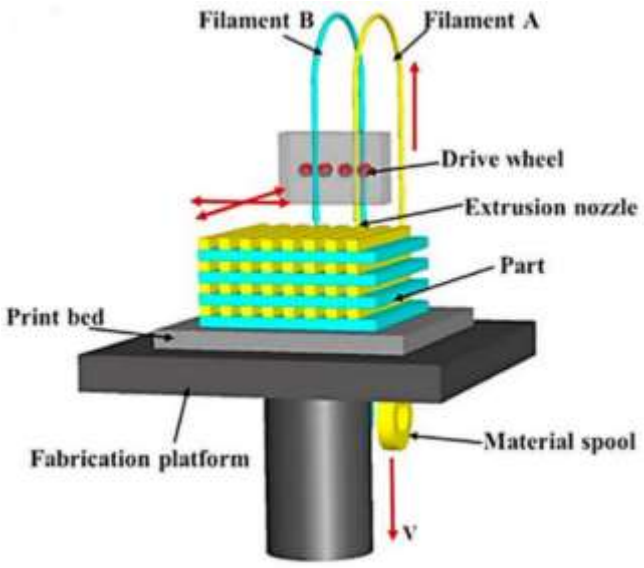

Figure 3.4 : Procedure for Fused Deposition Modelling.

The usage of semi-finished items, which may be made via extrusion, is a significant benefit of FDM. This feature should be used since it allows for the economical

modification and functionalization of materials. However, the deposition approach is a limiting element, which is acceptable when the structure is porous or the surface roughness is constrained [4].

3.4 Selective Laser Sintering

One of the most well-known 3D printing techniques is Selective Laser Sintering (SLS). Ross House holder first developed and patented selective laser sintering in 1979, but Carl Deckard's work at the University of Texas at Austin in the late 1980s led to its commercialization. Following that, Throughout the 1990s, both DTM and EOS pioneered the selective laser sintering method, which enabled the creation of complex cores and moulds for sand casting applications utilizing sand particles bonded with a polymer resin. DTM has applied the coated powder idea to metals, enabling the selective laser sintering machine to create powder metallurgy steel components in the green state [87]. Its popularity stems from the fact that SLS can manufacture parts in conventional polymers with acceptable mechanical properties [75].

Amorphous thermoplastics have a much wider softening range than semi-crystalline thermoplastics. Polymer processing must be carried out at a steady ambient temperature. The laser is used to locally provide the melting energy, preventing the surrounding powder from becoming hotter. Throughout the building process, two parts (liquid and solid phases), exist simultaneously. For best processing, a material's melting and crystallization temperature ranges should be as high as feasible, with a minimum for the melting region to ensure that the material melts quickly when exposed to laser light. On the other hand, a high melting enthalpy is preferred due to the large activation energy necessary, since this results in excellent separation of the liquid and solid parts [4].

The main advantage of SLS is its low cost, especially for small-sized items. It may be utilized for prototypes, support components, and small series items [75]. Nevertheless, a significant limitation of this approach has been a restricted spectrum of appropriate materials, owing to the components available not being in the correct powdered state for manufacture [4]. Figure 3.5 shows a model of the selective laser sintering method.

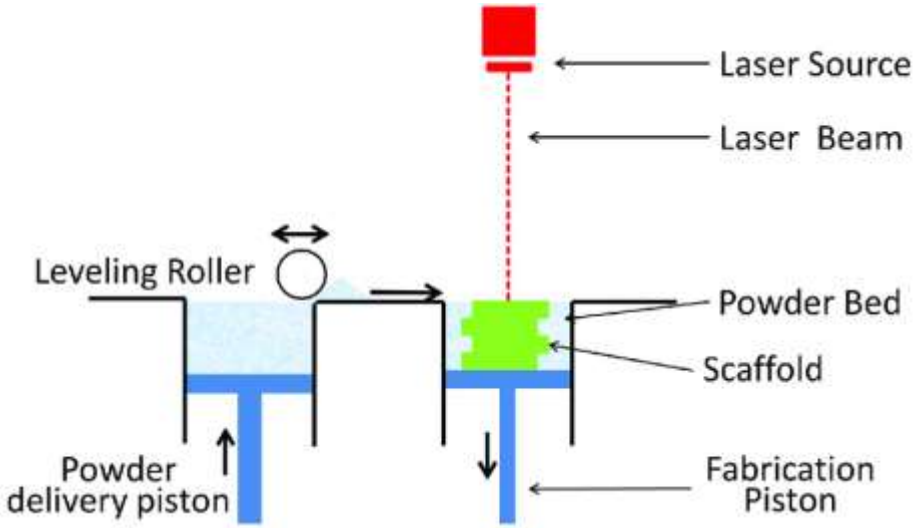

Figure 3.5 : Procedur for Selective Laser Sintering.

4. CERAMIC PARTS IN VAT PHOTOPOLYMERIZATION

Vat photopolymerization (Digital Light Processing or Stereolithography) is acknowledged as the most significant Additive Manufacturing (AM) approach in terms of dimensional precision, since this process can fabricate parts with great resolutions down to the micrometer range, low tolerances, and high surface quality [89]. The preparation of the suspension, which is composed of monomers, photoinitiators, and ceramic powder, is an crucial step in the Vat photopolymerization of ceramics [90]. In such slurries, the interaction between monomers and photoinitiators is generally based on photopolymerization, resulting in the formation of a polymeric structure. (If the monomers have multiple functions, cross-linking will occur.) [90]. A photocurable suspension may also contain light absorbers, defoamers, plasticizers, dispersants, and diluents.

In order to be used in vat polymerization, the ceramic powder or ceramic powder combination must meet some process requirements [90]. As producing a high-quality ceramic is the aim, the freeform ceramic green body needs to be highly dense, either for its refractory qualities or so that it may be easily sinterable to produce a dense ceramic. The photopolymerisable medium must contain ceramic particles that are homogeneously and efficiently dispersed, and the particles must be stable without significant segregation for a sufficient amount of time (e.g. hours to days). Unstable suspensions with rapid segregation could lead to material inhomogeneity in the fabricated parts. In order to maintain adequate flow during the printing process, a good candidate for a ceramic suspension should also maintain a sufficient viscosity [91].

In addition to all these, it may be possible to create a suitable and quality product for 3D printing by using ceramic powders in the resin in various chemicals that support it. The ceramic resin must satisfy a variety of specifications, including having a viscosity that is low enough to enable self-leveling and layer recoating, having a high ceramic particle loading to enable densification of the sintered parts, and having an adequate cure depth to enable strong interlayer adhesion during printing [89]. At the same time, several components are included in ceramic resins used in 3D printing to ensure a

rheologically acceptable behavior and match these specifications. Diluents and dispersants are some of the components included in ceramic resins. The choice of diluent or dispersion elements has a significant impact on rheological characterisation and the solubility of solid particles in resin, even if it has no direct impact on the final object's dimensional or mechanical quality. The ratio of the monomer, dispersant, and diluent should be chosen based on the solid loading of the suspension [84].

The several chemicals are employed to reduce the viscosity of the ceramic resin. Although diluents don't increase the mechanical toughness of the green printed parts, they do contribute to reducing the refractive index (RI) and giving the resin a low viscosity [84]. The refractive indexes of a few printed ceramics are shown in Table 4.1.Diluents also aid in reducing the polymeric phase's shrinkage tendency, which is frequently brought on by warping or delamination [79]. The homogeneity of a suspension depends critically on the liquid medium's affinity with ceramic particles [90]. The difunctional HDDA(1,6-Hexanediol diacrylate) is one of the monomers that is most frequently employed in ceramic lithographic printing due to its low viscosity and favorable cross-linking behavior [74,78]. In the same manner, This difunctional acrylate exhibits good agreement between diffusion-controlled degradation during debinding [90]. To enhance mechanical characteristics and crosslinking during the printing process, HDDA can be utilized in combination with tri- or tetrafunctional monomers [89].

Table 4.1 : Refractive index for some printable ceramic materials.

Ceramic	Refractive Index (RI)
Alumina (Al_2O_3)	1.52 – 1.70
Silica (SiO_2)	1.56
Zirconia (ZrO_2)	2.176 – 2.20
PZT	2.50
Silicon Nitride (Si_3N_4)	2.10

During ceramic powder works, pre-treatment applications are made to support the mixing of the powders with the slurries homogeneously and without agglomeration. Firstly, ceramic particles are previously mixed with the a solvent, (e.g. ethanol or acetone). Then stirred in a planetary mill, ball mill, or ultrasonic mixer. This process also homogenizes the particle size of the ceramic particles while preventing

agglomeration. Finally, the powder is dried to remove the solvent, and while the product is being prepared, the ceramic mixture is added with a dipersant so that it is homogeneously dispersed in the slurry.

Dispersants are one of the important issues for ceramic suspensions. Through favoring the mixing phase in a proper dispersion of the powder in solution, this type of component avoids the rapid sedimentation of the solid suspension [84]. In addition, dipersants prevent agglomeration. Ceramic particles having many hydroxyl groups on their surfaces have a strong tendency to agglomerate, which increases the suspension viscosity. The dispersant's function is to decrease this attraction by an adsorption process since the Van der Waals attraction between particles rises with interparticle distance. As dispersants' type and quantity have a considerable impact on the rheological behavior and stability of suspensions, they can improve the manufactureability of highly loaded ceramic slurries [90]. The most widely used ceramics, such alumina, zirconia, and silica, contain a hydroxyl group on their surface that gives them a hydrophilic behavior that makes them easy to agglomerate depending on the size of the particles [65]. It has to be highlighted that the optimal point of minimal viscosity for dispersant addition exists. A small amount of dispersant may not completely cover the particle surface, which might lead to flocculation [55, 31]. Table 4.2 presents a list of dispersants that have been widely used in the literature.

Table 4.2 : Dispersants used in formulations of ceramic slurries for vat photopolymerization.

Dispersant Name	Chemical Description
DisperBYK (BYK-Chemie)	A solution of an alkylammonium salt of a low-molecular-weight polycarboxylic acid polymer
BYK-w 969 (BYK-Chemie)	A solution of a hydroxy-functional alkylammonium salt of an acidic copolymer
DisperBYK-103 (BYK-Chemie)	A solution of a copolymer with filler affinic groups
DisperBYK-111 (BYK-Chemie)	Copolymer with an acid group
Variquac CC 42 NS (Evonik)	Polypropoxy quaternary ammonium chloride.
Triton X-100 (Sigma-Aldrich)	A non-ionic surfactant called octylphenol ethoxylate has an aromatic hydrocarbon hydrophobic group and a hydrophilic polyethylene oxide chain.

5. MATERIAL AND METHOD

5.1 Chemicals

5.1.1 KER 828

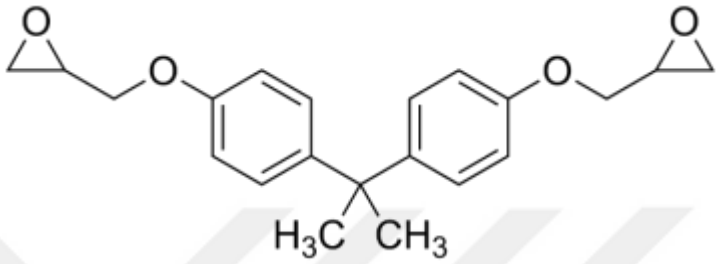

Figure 5.1 : Chemical structure of KER 828.

KER 828 was supplied by Sigma Aldrich and used as received. The chemical formula of KER 828 is $C_{21}H_{24}O_4$. Its viscosity and density are 12 ~ 14 Pa.s, 1.16 kg/L, respectively. Epoxy group content is 5260 - 5420 mmol/kg. Its molar mass is 184.5-190.0 g/eq The CAS number of KER 828 is 25068-38-6. Chemical structure of KER 828 is shown in Figure 5.1.

5.1.2 Hydroquinone

Figure 5.2 : Chemical structure of Hydroquinone.

Hydroquinone was supplied by Sigma Aldrich. This chemical substance was used without any treatment. The chemical formula of hydroquinone is C_6H_6O. Its molar mass is 110.11 g/mol. The CAS number of hydroquinone is 123-31-9. Chemical structure of hydroquinone is shown in Figure 5.2.

5.1.3 Triphenylphosphine

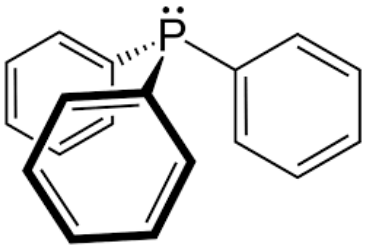

Figure 5.3 : Chemical structure of triphenylphosphine.

Triphenylphosphine was supplied by Sigma Aldrich. This chemical substance was used without any treatment. The chemical formula of triphenylphosphine is $C_{18}H_{15}P$. Its molar mass is 262.29 g/mol. The CAS number of triphenylphosphine is 603-35-0. Chemical structure of triphenylphosphine is shown in Figure 5.3.

5.1.4 Acrylic acid

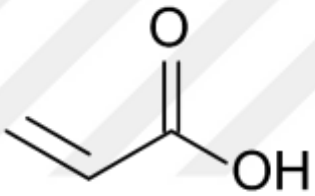

Figure 5.4 : Chemical structure of acrylic acid.

Acrylic acid was supplied by Sigma Aldrich. This chemical substance was used without any treatment. The chemical formula of acrylic acid is $C_3H_4O_2$. Its molar mass is 72.06 g/mol. The CAS number of acrylic acid is 79-10-7. Chemical structure of acrylic acid is shown in Figure 5.4.

5.1.5 Potassium hydroxide

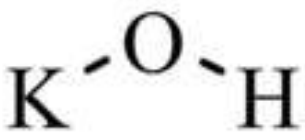

Figure 5.5 : Chemical structure of potassium hydroxide.

Potassium hydroxide was supplied by Sigma Aldrich. This chemical substance was used without any treatment. The chemical formula of potassium hydroxide is KOH.

Its molar mass is 56.1056 g/mol. The CAS number of potassium hydroxide is 1310-58-3. Chemical structure of potassium hydroxide is shown in Figure 5.5.

5.1.6 Phenolphthalein

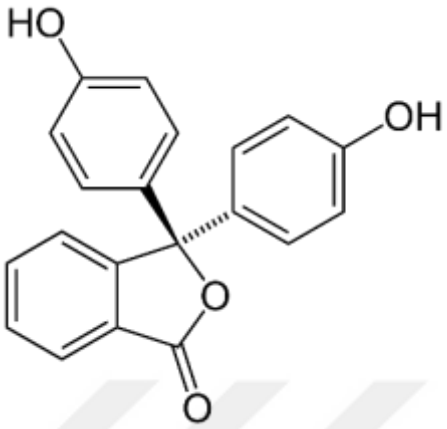

Figure 5.6 : Chemical structure of phenolphthalein.

Phenolphthalein was supplied by Sigma Aldrich. This chemical substance was used without any treatment. The chemical formula of phenolphthalein is $C_{20}H_{14}O_4$. This chemical substance molar mass is 318.32 g/mol. The CAS number of phenolphthalein is 77-09-8. Chemical structure of phenolphthalein is shown in Figure 5.6.

5.1.7 Chloroform

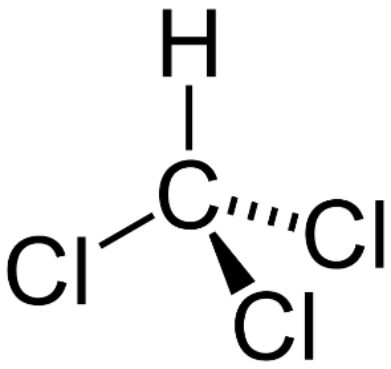

Figure 5.7 : Chemical structure of chloroform.

Chloroform was supplied by Carlo Erba. This chemical substance was used without any treatment. The chemical formula of chloroform is $CHCl_3$. This chemical substance molar mass is 119.38 g/mol. The CAS number of chloroform is 67-66-3. The density of chloroform, a widely used organic solvent, is 1.4832 g/mL at 20 °C. Chemical structure of chloroform is shown in Figure 5.7.

5.1.8 Ethyl alcohol

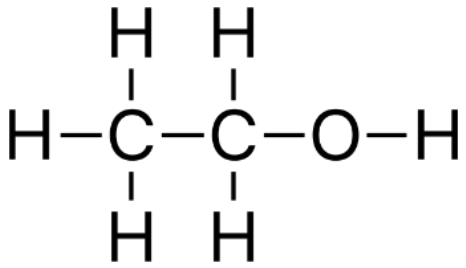

Figure 5.8 : Chemical structure of ethyl alcohol.

Ethyl alcohol was supplied by Sigma Aldrich. This chemical substance was used without any treatment. The chemical formula of ethyl alcohol is C_2H_6O. This chemical substance molar mass is 46.07 g/mol. The CAS number of ethyl alcohol is 64-17-5. Chemical structure of ethyl alcohol is shown in Figure 5.8.

5.1.9 1,6-Hexanediol diacrylate

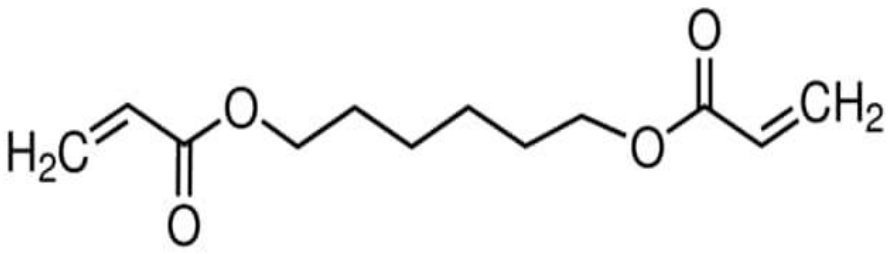

Figure 5.9 : Chemical structure of 1,6-Hexanediol diacrylate.

1,6-Hexanediol diacrylate was supplied by Sigma Aldrich. This chemical substance was used without any treatment. The chemical formula of 1,6-hexanediol diacrylate is $C_{12}H_{18}O_4$. This chemical substance molar mass is 226.27 g/mol. The CAS number of 1,6-hexanediol diacrylate is 13048-33-4. Chemical structure of 1,6-hexanediol diacrylate is shown in Figure 5.9.

5.1.10 BYK W-969

BYK W-969 was supplied by BYK Chemie. This chemical substance was used without any treatment. BYK W-969 is a solution of a hydroxy-functional alkylammonium salt of an acidic copolymer. Acts as monofunctional, deflocculating wetting and dispersing agents. It wets the filler particles and lead to a moderate interaction of the particles. This additive can be crosslinked into the polymer matrix because of its OH functionality. It improves the wetting and dispersing rate of fillers

during dispersion and dramatically reduces viscosity, so that higher filler loading is possible.

5.1.11 Di-trimethylolpropane tetraacrylate

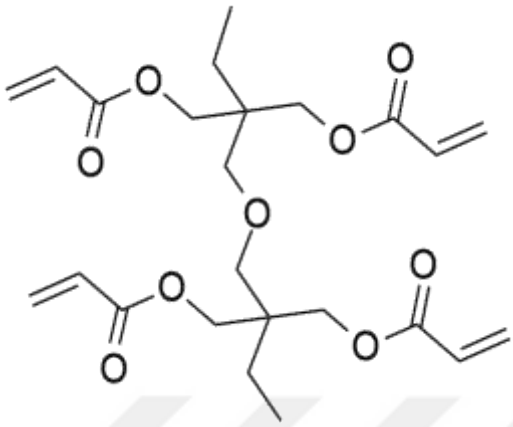

Figure 5.10 : Chemical structure of SR355.

Di-trimethylolpropane tetraacrylate (SR355) was supplied by Sartomer. This chemical substance was used without any treatment. The chemical formula of di-trimethylolpropane Tetraacrylate is $C_{24}H_{34}O_9$. This chemical substance molar mass is 466.5 g/mol. The CAS number of di-trimethylolpropane tetraacrylate is 94108-97-1. Chemical structure of SR355 is shown in Figure 5.10.

5.1.12 2-Hydroxy-2-methyl-1-phenyl-propan-1-one

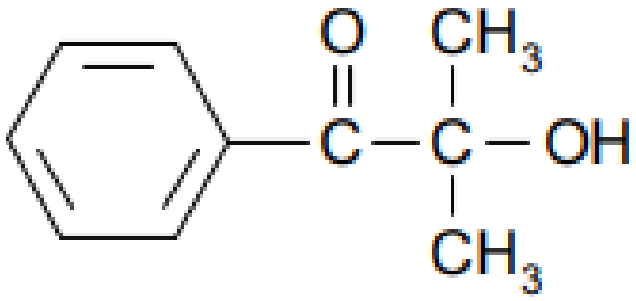

Figure 5.11 : Chemical structure of Darocur 1173.

Darocur 1173 was supplied by Ciba. This chemical substance was used without any treatment. The chemical formula of darocur 1173 is $C_{10}H_{12}O_2$. This chemical substance molar mass is 164.2 g/mol. The CAS number of darocur 1173 is 7473-98-5. The light absorption (λmax) of this photoinitiator has 244 nm, 278 nm, 330 nm. Chemical structure of Darocur 1173 is shown in Figure 5.11.

5.1.13 Phenylbis(2,4,6-trimethylbenzoyl)phosphine oxide

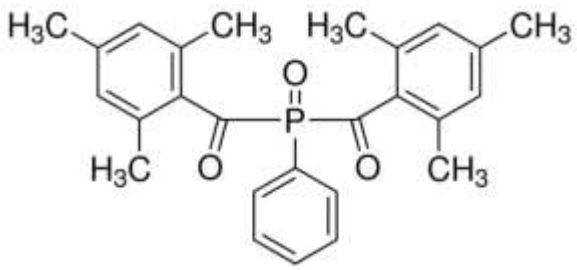

Figure 5.12 : Chemical structure of Phenylbis(2,4,6-trimethylbenzoyl)phosphine oxide.

Phenylbis(2,4,6-trimethylbenzoyl)phosphine oxide (BAPO) was supplied by Abcr. This chemical substance was used without any treatment. The chemical formula of phenylbis(2,4,6-trimethylbenzoyl)phosphine oxide is $C_{26}H_{27}O_3P$. This chemical substance molar mass is 418.46 g/mol. The CAS number of phenylbis(2,4,6-trimethylbenzoyl)phosphine oxide is 162881-26-7. The light absorption (λ_{max}) of this photoinitiator has 295 nm, 370 nm. Chemical structure of BAPO is shown in Figure 5.12.

5.1.14 Syloid Al – 1FP

Figure 5.13 : Silica powder.

Syloid Al-1FP (Silica Powder) was supplied by PEGE. This chemical substance was used without any treatment. The chemical formula of Syloid Al-1FP is SiO_2. This powder molar mass is 60.08 g/mol. The Partical size of this Syloid Al-1FP is 6.5 – 8.1 μm. Silica powder image is shown in Figure 5.13.

5.1.15 Zirconia powder

Zirconia Powder was supplied by Sigma Aldrich. This chemical substance was used without any treatment. The chemical formula of zirconia powder is ZrO_2. This powder molar mass is 123.218 g/mol. The Partical size of this zirconia powder is 25 μm.

5.1.16 Aluminum oxide powder

Aluminum oxide powder was supplied by Sigma Aldrich. This chemical substance was used without any treatment. The chemical formula of aluminum oxide powder is Al_2O_3. This powder molar mass is 101.960 $g \cdot mol^{-1}$. The Partical size of this aluminum oxide powder is 0.3 μm.

5.2 Equipment

5.2.1 Thermal gravimetric analysis

Perkin Elmer brand Pyris I TGA device was used to measure the thermo-oxidative stability of the prepared organic-inorganic hybrid materials. TGA analysis was carried out in inert conditions with a heating rate of 10 °C/min, between 30 °C and 900°C. Analysis results are shown in Section IV. Perkin Elmer brand Pyris I TGA analysis device is shown in Figure 5.14.

Figure 5.14 : Perkin Elmer brand Pyris I TGA.

5.2.2 Differential scanning calorimetry

Differential Scanning Calorimetry measurements were performed with a Perkin-Elmer Jade DSC, one run from -30 °C to 400°C with a heating rate of 10 °C·min^{-1} under inert conditions. Analysis results are shown in Section VI. Perkin Elmer brand Jade DSC analysis device is shown in Figure 5.15.

Figure 5.15 : Perkin-Elmer Jade DSC.

5.2.3 Scanning electron microscope

The fracture surface morphology of UV-cured organic-inorganic hybrid materials was imaged by Scanning Electron Microscope (SEM). Tescan Vega3 scanning electron microscope was used. Before examining the morphological images of the samples with scanning electron microscopy, the samples were coated with Au/Pd for 120 seconds in the coating device. Analysis results are shown in Section VI. Tescan Vega3 scanning electron microscope is shown in Figure 5.16.

Figure 5.16 : Tescan Vega3 Scanning Electron Microscope.

5.2.4 Mastersizer

The particle size measurement of the powder mixture, which was mixed with turbula and then ground with a Ball mill device for 6 hours and finally added to the binder, was measured with a Malvern brand mastersizer 2000 device. Analysis results are shown in Section VI. Malvern brand mastersizer 2000 analysis device is shown in Figure 5.17.

Figure 5.17 : Malvern mastersizer 2000.

5.2.5 Fourier-transform infrared spectroscopy

The molecular bond and functional group analysis of polymers were performed by FT-IR technique using a Perkin Elmer Spectum One FT-IR Spectrometer. Analysis results are shown in Section VI. FT-IR Spectrometer device is shown in Figure 5.18.

Figure 5.18 : Perkin Elmer Spectum One FT-IR Spectrometer.

5.3 Other devices

5.3.1 UV cabinet

The UV cabinet shown in Figure 5.19 was used to cure the prepared organic-inorganic hybrid formulations with UV. The UV cabinet has 3 electrical systems. The plate to

which the electrical system is connected has the ability to move up and down. High pressure UV lamp (OSRAM, 300W) was used as a UV light source in the system.

Figure 5.19 : UV cabinet and High pressure UV lamp (OSRAM, 300W).

5.3.2 Turbula

Using Turbula, 80% silica powder with 6.5 - 8.7 micron particle size, 15% zirconia powder with 5 micron particle size and 5% aluminum oxide powder with 0.5 micron particle size were mixed at constant speed for 1 hour. WAB T2F Turbula Heavy Duty Shaker-Mixer was used for this process. Turbula mixer is shown in Figure 5.20.

Figure 5.20 : WAB T2F Turbula Heavy Duty Shaker-Mixer.

5.3.3 Ball mill

A ball mill device was used to grind aluminum powder, silica powder and zircon powder of different particle sizes. While grinding the ceramic powder mixture, zircon mortar and balls were used. Fritsch brand Planetary Mono Mill PULVERISETTE 6 ball mill device is shown in Figure 5.21.

Figure 5.21 : Fritsch Planetary Mono Mill PULVERISETTE.

5.3.4 Ultrasonic homogenizer

Ultrasonic homogenizer is also known as sonicator. In these machines, the homogenization process is carried out by means of ultrasonic waves. It ensures that heterogeneous products are converted into homogeneous form as a result of mixing them by ultrasonic wave. While the resin, ceramic powder mixture and other chemicals were added, the mixing process was carried out with the help of an ultrasonic homogenizer. Bandelin brand SONOPULS HD 2070.2 device was used. The ultrasonic homogenizer used is shown in Figure 5.22.

Figure 5.22 : Bandelin SONOPULS HD 2070.2.

5.3.5 Evaporator

After the reactions carried out in the study, an evaporator device was used to remove the used solvent. The device works with the principle of removing the solvent in the resin by applying heat and vacuuming, and then collecting it in a separate container after cooling. The device used is Heidolph Laborota 4001 evaporator and is shown in Figure 5.23.

Figure 5.23 : Heidolph Laborota 4001 evaporator.

5.3.6 Teflon ® mold

Teflon mold was used to cure the products. The partitions on the Teflon mold shown in Figure 5.24. were designed and prepared to be 50 mm × 10 mm × 1 mm in size.

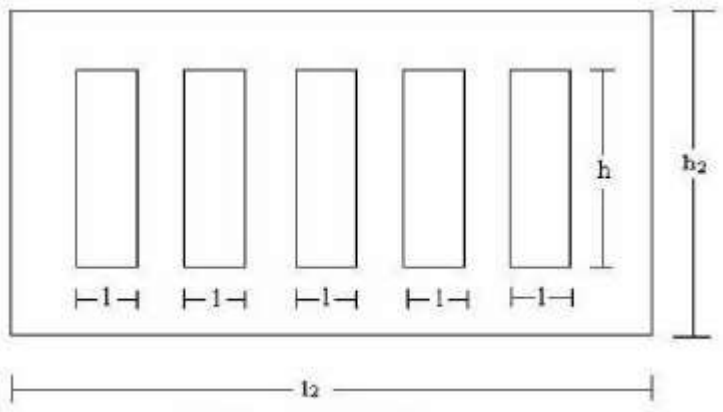

Figure 5.24 : Teflon® Mold Used to Prepare EAC samples.

5.4 Experimental

5.4.1 Preparation of epoxy acrylate oligomer

A three-necked 500 mL round-bottom flask with a nitrogen inlet and a dropping funnel was charged with 100 g of DGEBA epoxy resin (KER-828, epoxy group content: 5260–5420 mmol/kg), 0.19 g of hydroquinone, and 1.49 g of triphenylphosphine. The mixture was heated to 70 °C under nitrogen and stirred for 30 minutes. The setup of the apparatuses of the epoxy acrylate reaction is as shown in Figure 5.25. During the reaction, a color transition from green to yellow was observed in the three-necked round-bottom flask due to the chemicals reacting with the increase in temperature. The color transition observed in the reaction is shown in Figure 5.26. Then, dropwise add 69.62 mL of acrylic acid. The mixture of the reaction was maintained at 80 °C for 4 hours after the addition was finished completely. It was controlled by titration of 0.5 N KOH solution in the presence of phenolphthalein indicator. The liquid was viscous, clear, and yellow in color. The structure of EA was characterized by infrared spectroscopy.

Figure 5.25 : Reaction Setup.

Figure 5.26 The color transition observed in the reaction.

Chloroform and distilled water (1:1) mixture have been used for purification. A combination of distilled water and chloroform was used to purify the yellow, viscous liquid. As a scavenger agent, NaCl was utilized. After phase separation was observed, a separating funnel was used to separate the water phase from the chloroform phase. This proces was repeated by three times. The light yellow epoxy acrylate resin formed as a result of the reaction is shown in Figure 5.27. A representation of this reaction is shown in Figure 5.28.

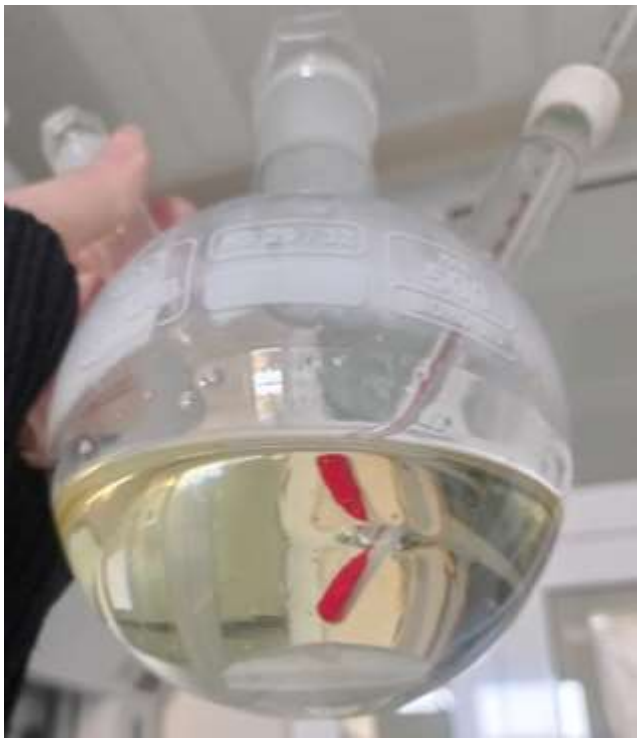

Figure 5.27 : The light yellow epoxy acrylate resin.

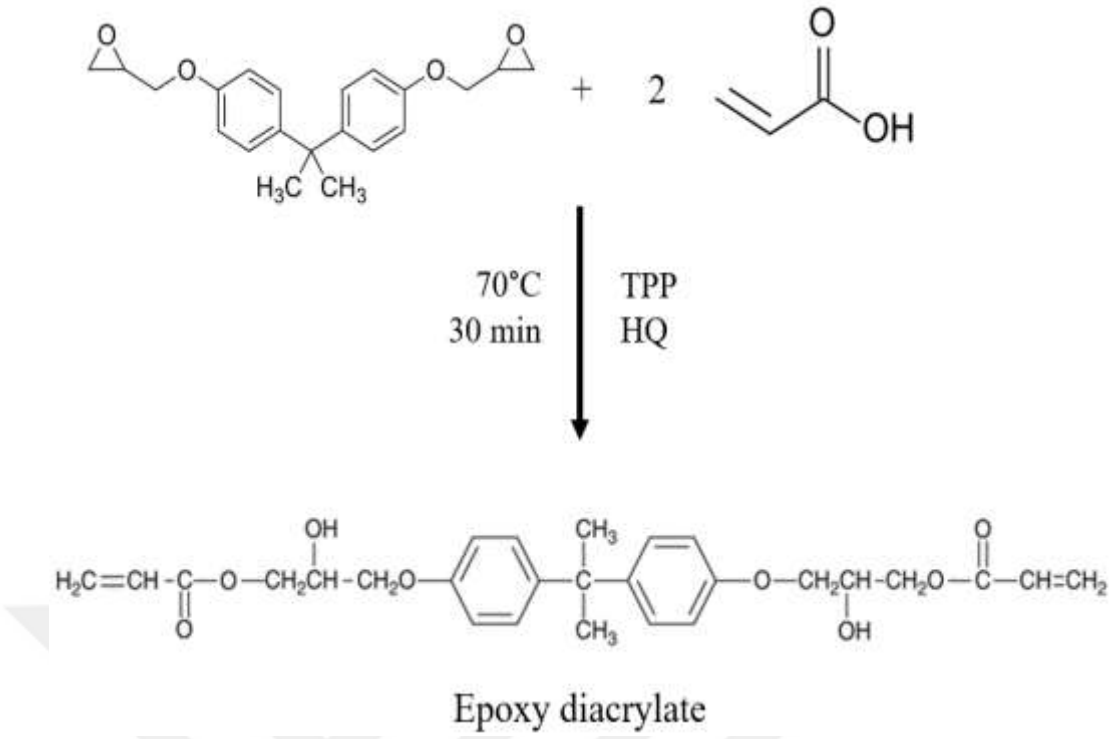

Figure 5.28 : A representation of Epoxy-Acrylate reaction.

5.4.2 Acid value titration

During the preparation of epoxy acrylate resin, the acid number of the polymerization system had to be constantly tested in order to ensure that the esterification reaction had fully completed. Titration method was used to measure the acid number. For the titration method, KOH-distilled water solution (0.5 N) was utilized. Initially, 0.5–1.0 g of epoxy - acrylate resin was carefully weighed into a conical flask.Then, 100 ml ethanol was used to dissolve the epoxy - acrylate resin. Finally, phenolphthalein indicator of 2 drops was added into the conical flask. Titration is continued until a pink color appears in the conical flask. The acid value is determined by the following equation.

$$\frac{\text{MKOH x VTitrant x FKOH x MWKOH x}}{\text{W}} = \text{Acid Value} \qquad (5.1)$$

In the above equation; M_{KOH} is the molarity of KOH, $V_{titrant}$ is the volume of KOH. W is the weight of the sample. F_{KOH} is the factor of KOH. MW_{KOH} is the molecular weight of the KOH (56.1 g/mol).

5.4.3 Powder preperation

A total of 30 grams of powder was weighed, including 80% silica powder with a particle size of 6.5 - 8.7 microns, 15% zirconia powder with a particle size of 5 microns, and 5% aluminum oxide powder with a particle size of 0.5 microns.The weighed powder was mixed for 1 hour with the help of Turbula. Then a slurry was prepared with the resulting homogeneous powder mixture and ethanol at 40% to 60%. Prepared slurry were added to a zircon mortar, which contained the twenty zircon balls. After that, the mixture was ball-milled using zirconia balls for 5 hours at 300 rpm in a planetary ball mill. During the ball mill process, the device is programmed to mill for 5 minutes, stop for 5 minutes. After completion of the ball-milled process, the suspension was dried in a vacuum oven at 60 °C for 1 hour.

5.4.4 Green body preperation

After the epoxy acrylate resin was prepared, five different 50 ml beakers were taken and 10 g of resin was weighed into each beaker. In order to protect the samples from the light, the beakers were covered with aluminum foil. To each beaker, 20 wt% HDDA (1,6 hexanediol diacrylate) was added as reactive diluent. It was mixed with the homogenizer for 1 minute. Ceramic powders was added to the mixed resin at 0%, 30%, 40% and 50% by weight. To each prepared sample, 3% dispersant was added according to the powder ratio. It was mixed for 1 more minute with the homogenizer.

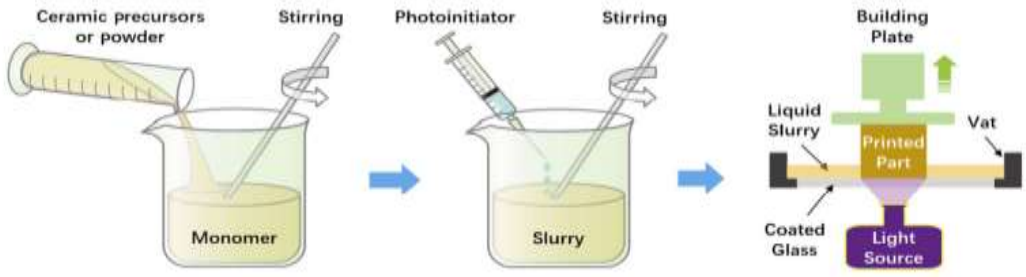

Figure 5.29 : Schematic illustration of steps involved in the photopolymerization-based AM of ceramic parts.

Then, SR355, a tetraacrylate derivative, was added as a crosslinker at a rate of 5% by weight of the epoxy-acrylate resin. Darocur 1173 and BAPO mixture used as UV photoinitiator system were added at 3% and 0.5%, respectively. The prepared slurry was mixed for 1 minute with the homogenizer. After the homogenization, prepared samples were poured on to a Teflon™ mold and before the curing process, covered

by a transparent film in order to prevent oxygen inhibition. At the end of process, the samples were cured with the high pressure UV lamp (OSRAM, 300 W) during 180 second. Schematic illustration of steps involved in the photopolymerization-based AM of ceramic parts is shown in Figure 5.29.

6. RESULT AND DISCUSSION

6.1 FTIR Analysis

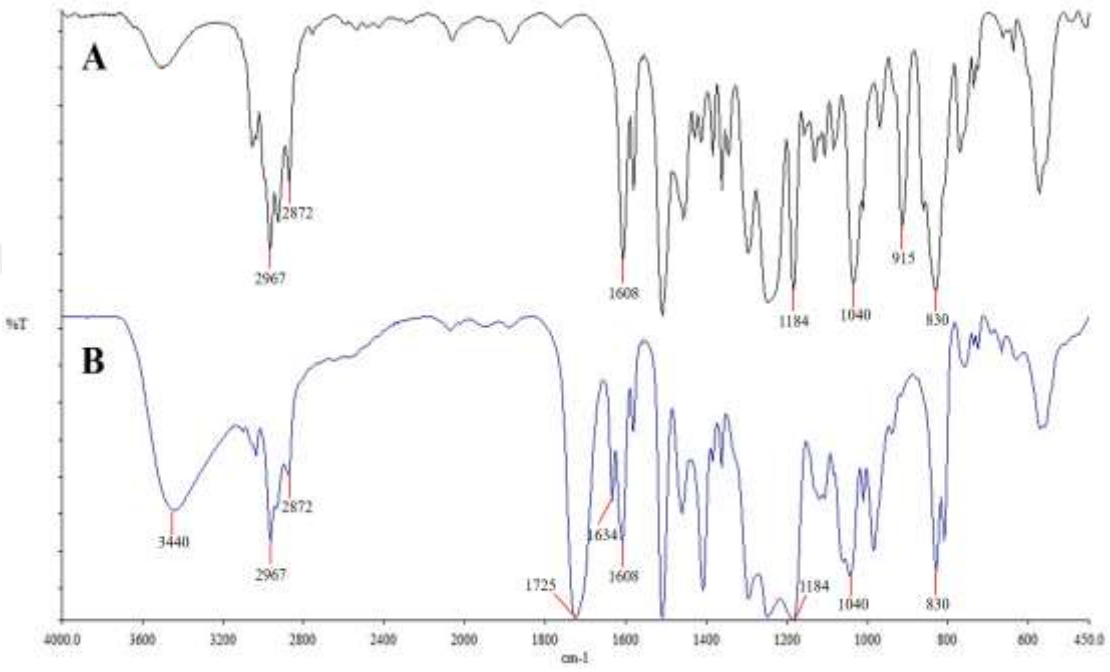

Figure 6.1 : FTIR spectra of the initial epoxy resin (A) and epoxy-acrylate resin (B).

The above spectrum is the comparative FTIR spectrum of initial epoxy resin and synthesized epoxy acrylate resin. The FTIR spectrum of the bisphenol A type epoxy resin (DGEBA) is shown in Figure 6.1A. Epoxy resin of the bisphenol A type has an unique -C-O deformation band at 915 cm^{-1} in the spectra. The peak observed at 1608 cm^{-1} corresponds to aromatic C=C stretching vibrations. The stretching vibration bands of CH_2 is appeared at 2967 cm^{-1}.

The FTIR spectrum of the epoxy-acrylate resin is typically shown in Figure 6.1B. It is clearly seen that the characteristic peak of the epoxy group observed at 915 cm^{-1} disappeared as a result of ring opening. The C=C stretching vibration results in absorption band in 1634 cm^{-1} for vinyl group. At 1725 cm^{-1} and 1184 cm^{-1}, respectively, two characteristic bands resulting from the C=O and C-O stretching vibrations are observed. Carbonyl groups in acrylic acid alone typically exhibit a sharp stretching vibration between 1700 and 1710 cm^{-1}. It should be known that this range

is carried to higher wave numbers (1725 cm^{-1}) in acrylated samples. The epoxy bands in the spectra of epoxy-acrylate resins are reduced as a result of the esterification process between the oxirane ring and acrylic acid. Strong broad band in 3200–3500 cm^{-1} regions corresponds to hydrogen bonded OH band.

6.2 Thermogravimetric Analysis

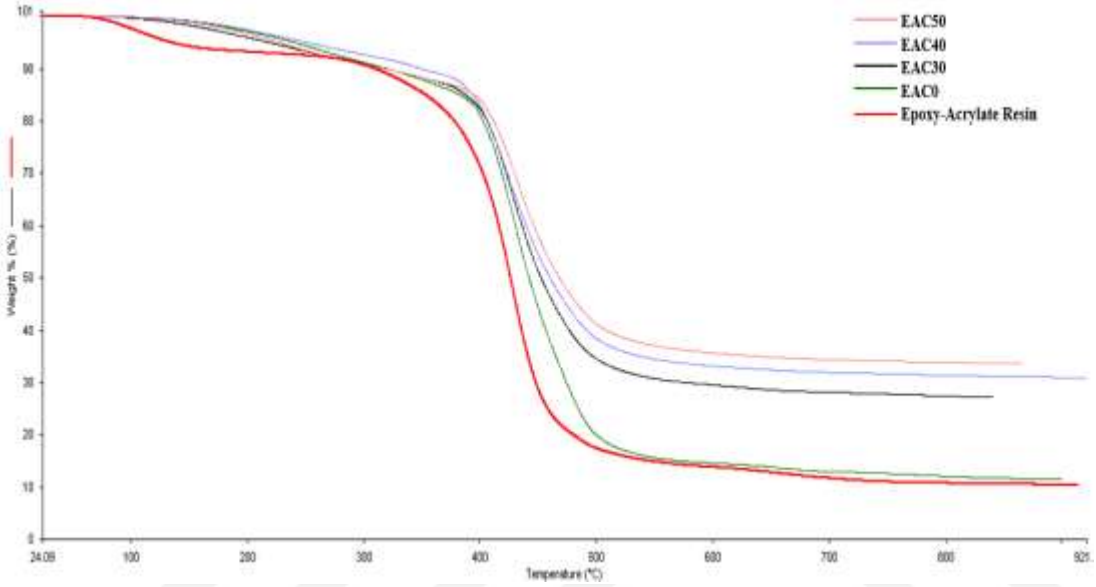

Figure 6.2 : TGA thermograms of cured EAC50, EAC40, EAC30, EAC0 and epoxy-acrylate resin.

Thermal stabilities of the cured EAC50, EAC40, EAC30, EAC0 were investigated by TGA method. The thermogravimetric analysis results show that the amount of ash increases along with the amount of inorganic additives in the resin. It was observed that the thermal resistance increased with the inorganic additive material. TGA thermograms of cured EAC50, EAC40, EAC30, EAC0 and epoxy-acrylate resin is shown in Figure 6.2.

6.3 Differential Scanning Calorimetry

Thermal transitions of the cured EAC30, EAC40 and EAC50 were investigated by DSC. According to EAC0 Differential Scanning Calorimetry measurements, the glass transition temperature value is 55.56 ºC, the ΔH value is 2.0394 J/g and the melting temperature value is 375.13 ºC as seen in Figure 6.3. DSC results are given in Table 6.1.

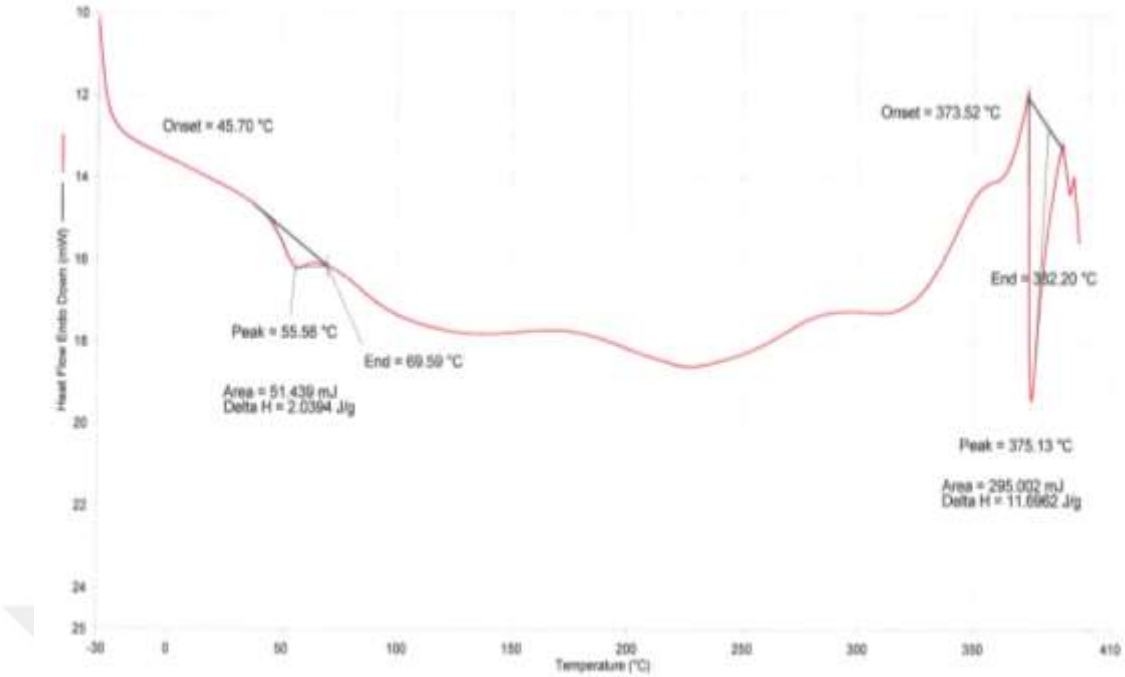

Figure 6.3 : DSC curve of EAC0.

According to EAC30 Differential Scanning Calorimetry measurements, the glass transition temperature value is 54.10 ºC, the ΔH value is 1.5321 J/g and the melting temperature value is 348.05 ºC as seen in Figure 6.4.

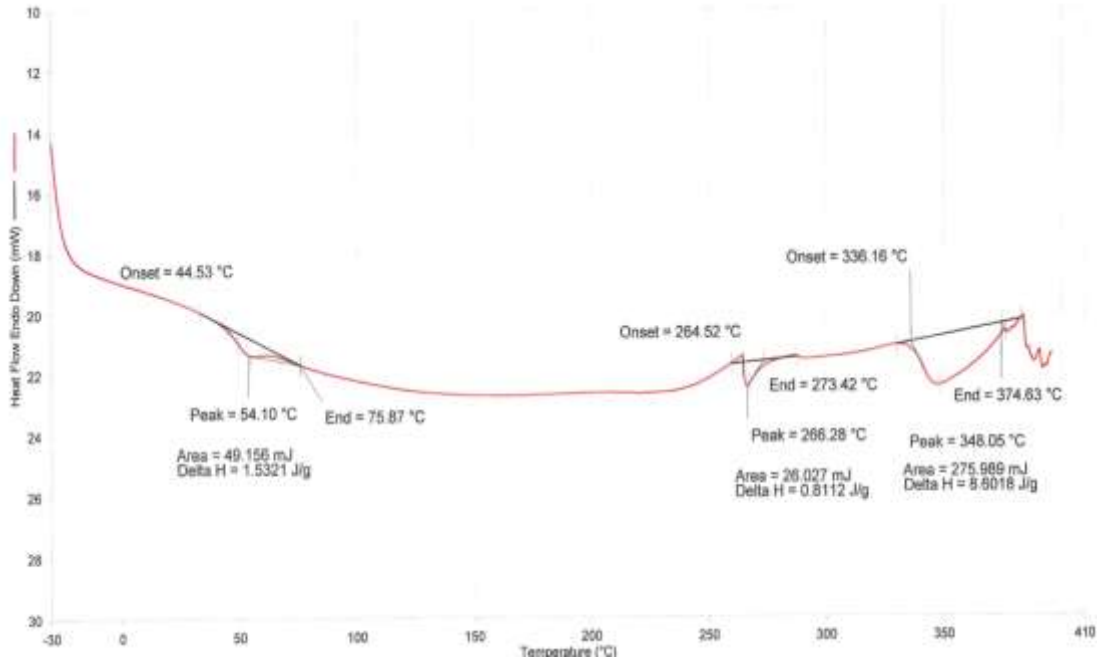

Figure 6.4 : DSC curve of EAC30.

According to EAC40 Differential Scanning Calorimetry measurements, the glass transition temperature value is 54.80 ºC, the ΔH value is 1.039 J/g and the melting temperature value is 346.23 ºC as seen in Figure 6.5.

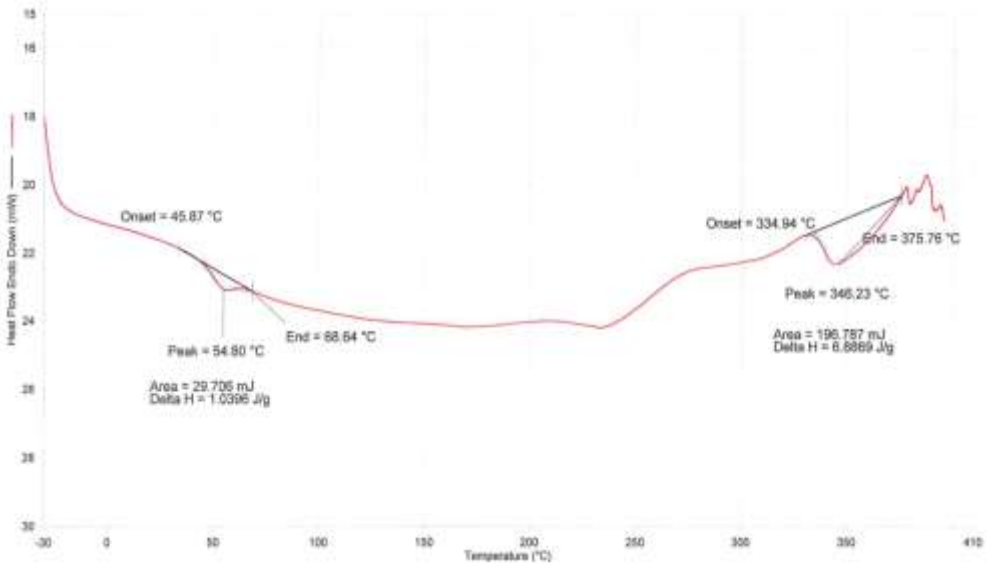

Figure 6.5 : DSC curve of EAC40.

According to EAC50 Differential Scanning Calorimetry measurements, the glass transition temperature value is 54.49 ºC, the ΔH value is 1.0628 J/g and the melting temperature value is 345.95 ºC as seen in Figure 6.6.

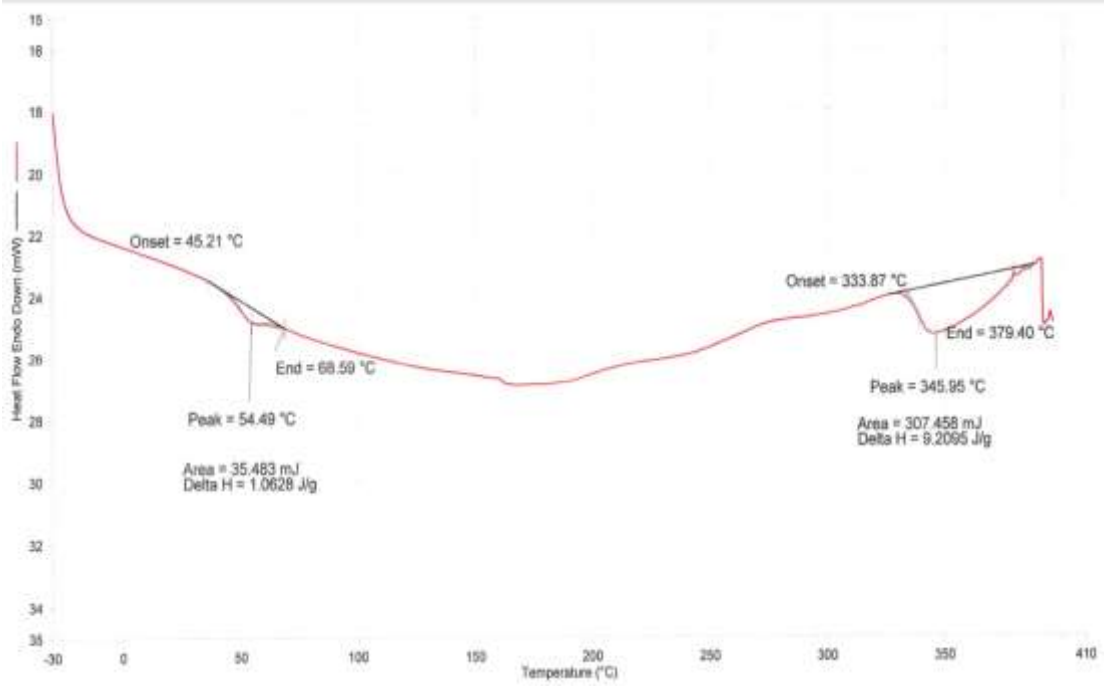

Figure 6.6 : DSC curve of EAC50.

Table 6.1 : DSC results for EAC0, EAC30, EAC40 and EAC50.

Code	Tg (ºC)	Tm (ºC)	ΔH (J/g)
EAC0	55.56	375.13	2.0394
EAC30	54.10	348.05	1.5321
EAC40	54.80	346.23	1.039
EAC50	54.49	345.95	1.0628

There was no noticeable difference between the glass transition temperature of the cured epoxy acrylate resin without inorganic additives and the glass transition temperature of the cured epoxy acrylate resins containing different amounts of additives. It was concluded that the added ceramic mixture had no effect on the glass transition temperature but resulted in a drop in the melting point of the cured epoxy acrylate.

6.4 Particle Size Distribution

Weighing a total of 30 grams of powder, consisting of 80% by weight silica powder with 6.5 - 8.7 micron particle size, 15% by weight zirconia powder with 5 micron particle size and 5% by weight aluminum oxide powder with 0.5 micron particle size, the powder mixture is first mixed with turbula and then ball mill process was applied. At the end of the ballmilled process, particle size measurement was made with a mastersizer device to find out the final powder size. As a result of the measurement, it was determined that the d(0.1) dimension of the powder mixture was 1.124 µm, the d(0.5) dimension was 2.328 µm and the d(0.9) dimension was 4.188 µm. Particle size measurement of ceramic mixture with mastersizer is shown in Figure 6.7.

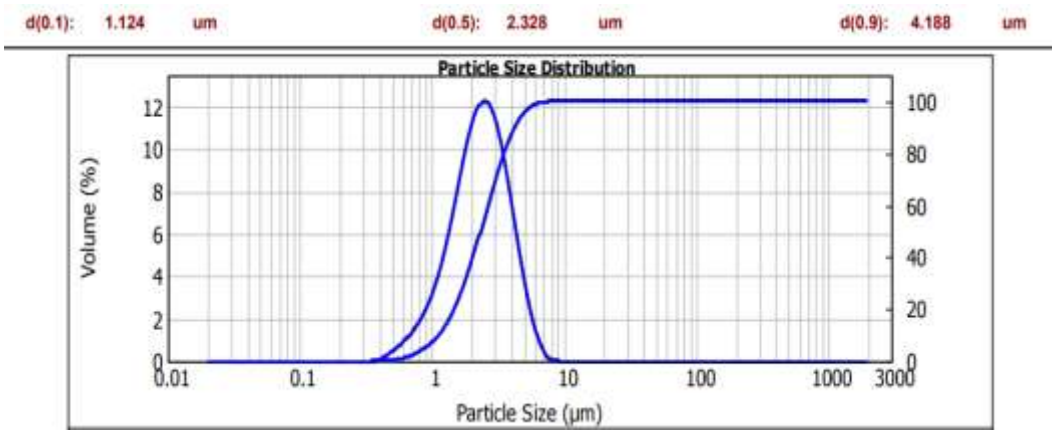

Figure 6.7 : Particle size measurement of ceramic mixture with mastersizer.

6.5 Scanning Electron Microscopy

SEM analysis was performed at different magnifications and with images taken from the fracture surfaces of the samples. SEM images of the EAC30 sample at 1 kx and 5 kx magnifications are shown in Figure 6.8 and Figure 6.9, respectively.

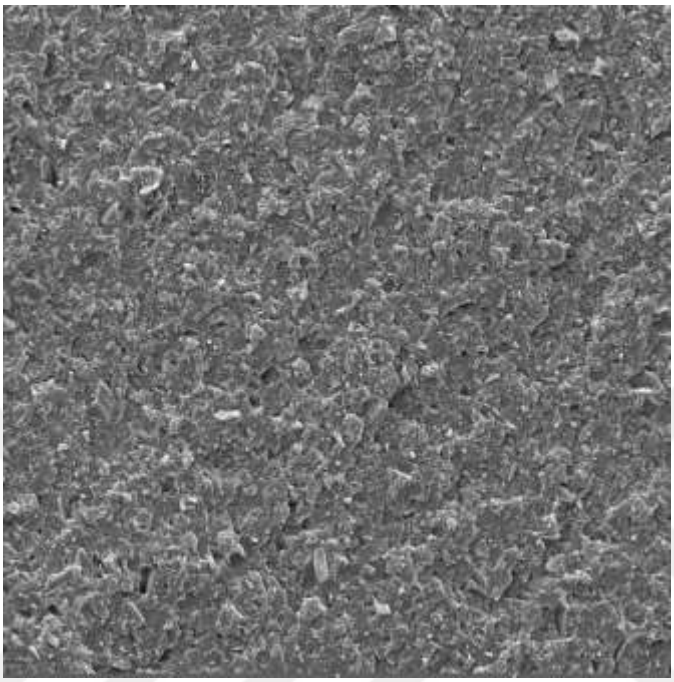

Figure 6.8 : SEM image of an EAC30 sample at 1 kx magnification.

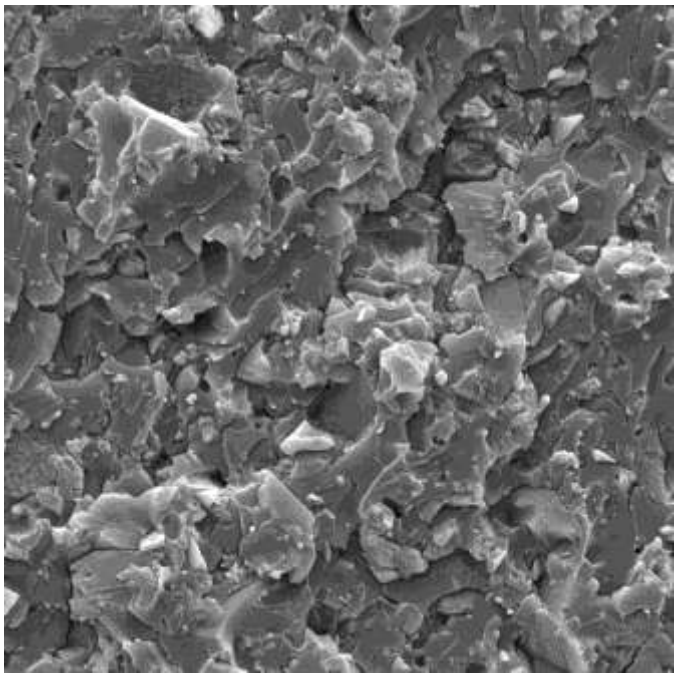

Figure 6.9 : SEM image of an EAC30 sample at 5 kx magnification.

SEM images of the EAC40 sample at 1 kx and 5 kx magnifications are shown in Figure 6.10 and Figure 6.11, respectively.

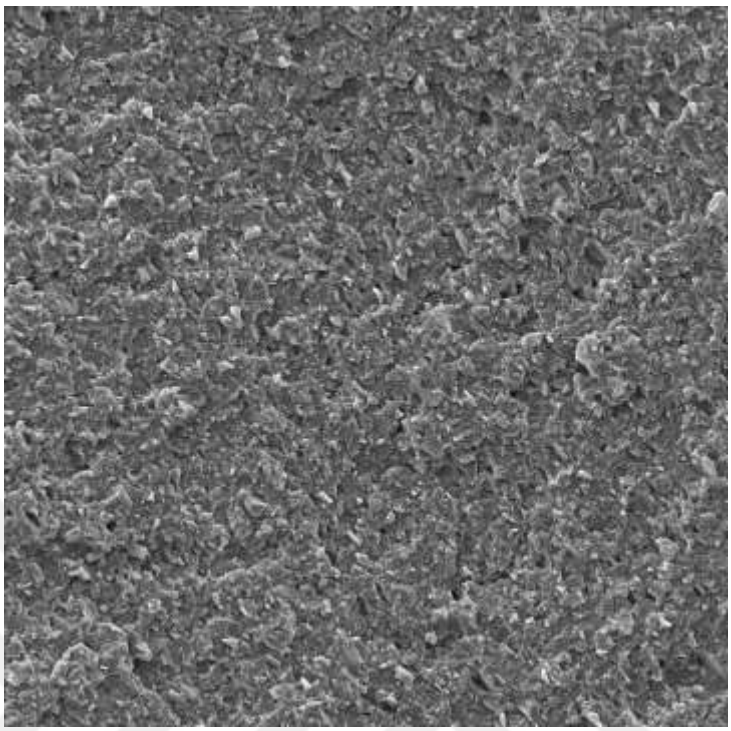

Figure 6.10 : SEM image of an EAC40 sample at 1 kx magnification.

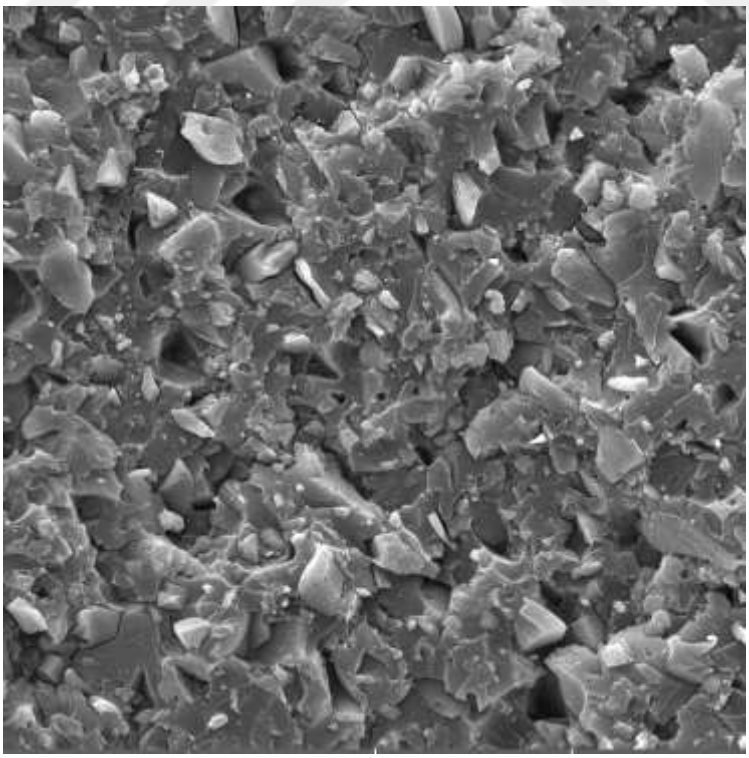

Figure 6.11 : SEM image of an EAC40 sample at 5 kx magnification.

SEM images of the EAC50 sample at 1 kx and 5 kx magnifications are shown in Figure 6.12 and Figure 6.13, respectively.

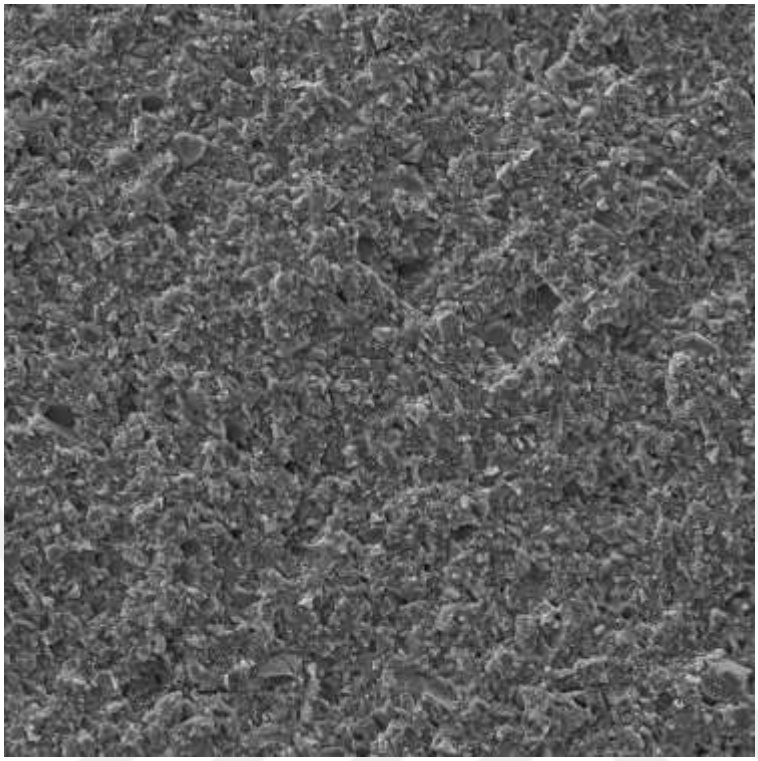

Figure 6.12 : SEM image of an EAC50 sample at 1 kx magnification.

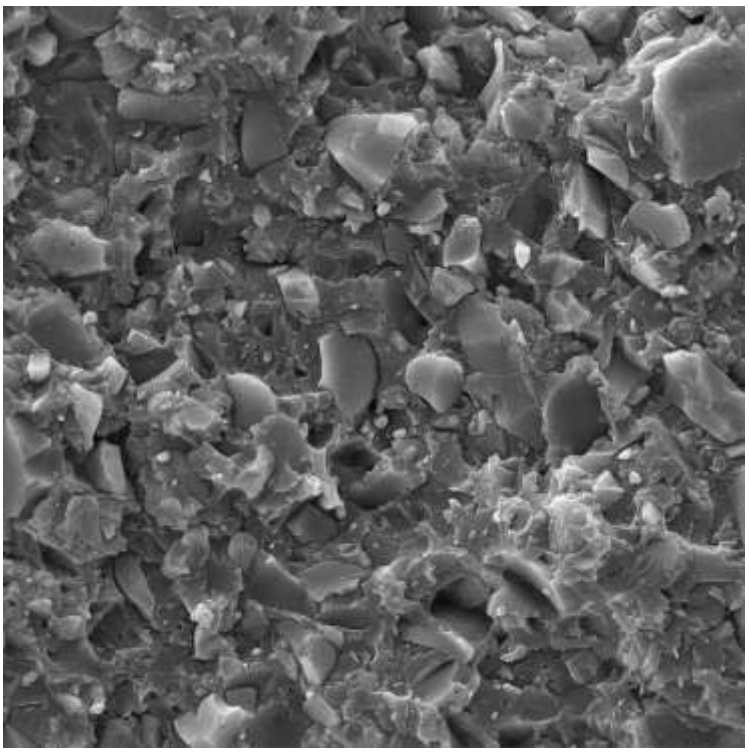

Figure 6.13 : SEM image of an EAC50 sample at 5 kx magnification.

7. CONCLUSION

In this thesis, studies were carried out on the resin system with ultraviolet light curable organic-inorganic hybrid structure to be used in 3D printing technology. In this context; The synthesis of UV light-curable epoxy acrylate resin, which has a completely organic structure, was carried out. In the synthesis process, bisphenol A type epoxy resin and acrylic acid as monomer, hydroquinone as inhibitor and triphenylphosphine as catalyst were used. The synthesized resin was characterized by Fourier-Transform Infrared Spectroscopy (FTIR). According to Fourier-Transform Infrared Spectroscopy results; It is clearly seen that the characteristic peak of the epoxy group observed at 915 cm^{-1} disappeared as a result of ring opening. The C=C stretching vibration results in absorption band in 1634 cm^{-1} for vinyl group. At 1725 cm^{-1} and 1184 cm^{-1}, respectively, two characteristic bands resulting from the C=O and C-O stretching vibrations are seen. Carbonyl groups in acrylic acid alone typically exhibit a sharp stretching vibration between 1700 and 1710 cm^{-1}. It should be known that this range is carried to higher wave numbers (1725 cm^{-1}) in acrylated samples. The epoxy bands in the spectra of epoxy-acrylate resins are reduced as a result of the esterification process between the oxirane ring and acrylic acid. Strong broad band in 3200–3500 cm^{-1} regions corresponds to hydrogen bonded OH band. As a result of the peaks observed in the spectrum, it was decided that the epoxy acrylate resin was successfully synthesized. In addition, the peaks seen in the FTIR spectrum were compared with other commercial epoxy acrylate resins with the help of the Know it all library in TÜBİTAK to ensure the accuracy of the synthesis.

The next stage of the thesis work was the preparation of the inorganic parts of the light-curable greenbody samples with an organic-inorganic hybrid structure. Silicon dioxide with particle size of 6.5-8.7 micron, zirconium with particle size of 25 micron and aluminum powder with particle size of 0.5 micron were prepared as 80%, 15% and 5% (w/v), respectively. It was mixed with turbula and ground with a planetry ballmill. At the end of the ballmilled process, particle size measurement was made with a

mastersizer device to find out the final powder size. As a result of the measurement, it was determined that the d(0.1) dimension of the powder mixture was 1.124 μm, the d(0.5) dimension was 2.328 μm and the d(0.9) dimension was 4.188 μm.

In the final stage of the study, five different green body samples were prepared. During the preparation of the samples, firstly synthesized EA (Epoxy Acrylate) resin, 20 wt% HDDA (1,6 hexanediol diacrylate), 3 wt% BYK W-969 (dispersant), 5 wt% SR355 (crosslinker), 3 wt% Darocur 1173 (Liquid photoinitiator) and 5 wt% BAPO (powder photoinitiator) was mixed with a Homogenizer. The ceramic powder mixture to be added as inorganic part later was added as 0 wt%, 30 wt%, 40 wt% and 50 wt% by weight. The samples were poured into a Teflon mold and the samples were cured with the high pressure UV lamp (OSRAM, 300 W) during 180 second. The cured samples were given the codes EAC0, EAC30, EAC40 and EAC50. Cured samples with organic-inorganic hybrid structure were characterized by TGA, DSC, SEM.

The thermogravimetric analysis (TGA) results show that the amount of ash increases along with the amount of inorganic additives in the resin. It was observed that the thermal resistance increased with the inorganic additive material.

In the Differential Scanning Calorimeter (DSC) graph of EAC0, it was seen that the glass transition temperature (Tg) value was 55.56 ºC, the ΔH value was 2.0394 J/g and the Tm value of the EAC0 was 375.13 ºC. In the DSC graph of the EAC30, the glass transition temperature (Tg) value was 54.10 ºC, the ΔH value was 1.5321 J/g, and the Tm value of the EAC30 was 348.05 ºC. It was observed in the DSC graph of EAC40 that the glass transition temperature (Tg) value was 54.80 ºC, the ΔH value was 1.0396 J/g and the melting temperature (Tm) value of EAC40 was 346.23 ºC. In the DSC graph of EAC50, it was seen that the glass transition temperature (Tg) value was 54.49 ºC, the ΔH value was 1.0628 J/g and the Tm value of EAC50 was 345.95 ºC. There was no noticeable difference between the glass transition temperature of the cured epoxy acrylate resin without inorganic additives and the glass transition temperature of the cured epoxy acrylate resins containing different amounts of additives. It was concluded that the added ceramic mixture had no effect on the glass transition temperature.

Scanning Electron Microscope (SEM) analysis was performed at different magnifications and with images taken from the fracture surfaces of the samples.

According to the results of the SEM analysis, the homogeneous hybrid network was successfully formed. The ceramic powder network is attached to the organic network at the molecular level.

As a result, epoxy acrylate resin was successfully synthesized in this thesis. This novel material which that prepared with epoxy acrylate resin, has an inorganic organic hybrid structure that can be cured with UV and is suitable for use in 3D printing technology.

REFERENCES

[1] **Barner-Kowollik, C., Bastmeyer, M., Blasco, E., Delaittre, G., Müller, P., Richter, B., & Wegener, M.** (2017). 3D laser micro-and nanoprinting: challenges for chemistry. Angewandte Chemie International Edition, 56(50), 15828-15845.

[2] **Jungst, T., Smolan, W., Schacht, K., Scheibel, T., & Groll, J.** (2016). Strategies and molecular design criteria for 3D printable hydrogels. Chemical reviews, 116(3), 1496-1539.

[3] **Murphy, S. V., & Atala, A.** (2014). 3D bioprinting of tissues and organs. Nature biotechnology, 32(8), 773-785.

[4] **Wendel, B., Rietzel, D., Kühnlein, F., Feulner, R., Hülder, G., & Schmachtenberg, E.** (2008). Additive processing of polymers. Macromolecular materials and engineering, 293(10), 799-809.

[5] **Bagheri, A., & Jin, J.** (2019). Photopolymerization in 3D printing. *ACS Applied Polymer Materials*, *1*(4), 593-611.

[6] **Zhang, J., & Xiao, P.** (2018). 3D printing of photopolymers. Polymer Chemistry, 9(13), 1530-1540.

[7] **Fu, J., Yin, H., Yu, X., Xie, C., Jiang, H., Jin, Y., & Sheng, F.** (2018). Combination of 3D printing technologies and compressed tablets for preparation of riboflavin floating tablet-in-device (TiD) systems. International journal of pharmaceutics, 549(1-2), 370-379.

[8] **Ligon, S. C., Liska, R., Stampfl, J., Gurr, M., & Mülhaupt, R.** (2017). Polymers for 3D printing and customized additive manufacturing. *Chemical reviews*, *117*(15), 10212-10290.

[9] **Zarek, M., Layani, M., Cooperstein, I., Sachyani, E., Cohn, D., & Magdassi, S.** (2016). 3D printing of shape memory polymers for flexible electronic devices. *Advanced Materials*, *28*(22), 4449-4454.

[10] **Liska R, Schuster M, Inführ R et al** (2007) Photopolymers for rapid prototyping. J Coat Technol Res 4:505–510. https://doi.org/10.1007/s11998-007-9059-3

[11] **Arsu, N., Aydin, M., Yagci, Y., Jockusch, S., & Turro, N. J.** (2006). One component thioxanthone based Type II photoinitiators. *Photochemistry and UV curing: new trends*, *1*, 17-29.

[12] **Bean, A. J.** (1992). Radiation curing of printing inks. *Radiation Curing: Science and Technology*, 301-332.

[13] **Chaudhary, R., Fabbri, P., Leoni, E., Mazzanti, F., Akbari, R., & Antonini, C.** (2022). Additive manufacturing by digital light processing: a review. *Progress in Additive Manufacturing*, 1-21.

[14] **Yagci, Y., Jockusch, S., & Turro, N. J.** (2010). Photoinitiated polymerization: advances, challenges, and opportunities. *Macromolecules*, *43*(15), 6245-6260.

[15] **Fouassier, J. P., & Lalevée, J.** (2012). *Photoinitiators for polymer synthesis: scope, reactivity, and efficiency*. John Wiley & Sons.

[16] **Berberoğlu, B.** (2020). *Ultraviyole Işıkla kürlenebilen Organik-Inorganik Hibrit Malzemelerin Sentezi Ve Karakterizasyonu* (Doctoral dissertation, Marmara Universitesi (Turkey)).

[17] **Jain, A., Blum, C., & Subramaniam, V.** (2009). Fluorescence lifetime spectroscopy and imaging of visible fluorescent proteins. In Advances in Biomedical Engineering (pp. 147-176). Elsevier.

[18] **Drobny, J. G**. (2010). Radiation technology for polymers. CRC press.

[19] **Tasic, S., Bozic, B., & Dunjic, B.** (2004). Synthesis of new hyperbranched urethane-acrylates and their evaluation in UV-curable coatings. *Progress in Organic Coatings*, *51*(4), 320-327.

[20] **Koleske, J. V.** (2002). Radiation curing of coatings (No. 45). West Conshohocken, PA: ASTM international.

[21] **Crivello, J. V., & Mao, Z.** (1997). Preparation and Cationic Photopolymerization of Organic− Inorganic Hybrid Matrixes. Chemistry of materials, 9(7), 1562-1569.

[22] **Rasaki, S. A., Xiong, D., Xiong, S., Su, F., Idrees, M., & Chen, Z.** (2021). Photopolymerization-based additive manufacturing of ceramics: A systematic review. *Journal of Advanced Ceramics*, *10*, 442-471.

[23] **Boddapati, A., Rahane, S. B., Slopek, R. P., Breedveld, V., Henderson, C. L., & Grover, M. A.** (2011). Gel time prediction of multifunctional acrylates using a kinetics model. *Polymer*, *52*(3), 866-873.

[24] **Ligon-Auer, S. C., Schwentenwein, M., Gorsche, C., Stampfl, J., & Liska, R.** (2016). Toughening of photo-curable polymer networks: a review. *Polymer Chemistry*, *7*(2), 257-286.

[25] **Kim, L. U., Kim, J. W., & Kim, C. K.** (2006). Effects of molecular structure of the resins on the volumetric shrinkage and the mechanical strength of dental restorative composites. *Biomacromolecules*, *7*(9), 2680-2687.

[26] **Hull, C. W., Spence, S. T., Lewis, C. W., Vinson, W., Freed, R. S., & Smalley, D. R.** (1998). *U.S. Patent No. 5,772,947*. Washington, DC: U.S. Patent and Trademark Office.

[27] **Moraes, R. R., Garcia, J. W., Barros, M. D., Lewis, S. H., Pfeifer, C. S., Liu, J., & Stansbury, J. W.** (2011). Control of polymerization shrinkage and stress in nanogel-modified monomer and composite materials. *Dental Materials*, *27*(6), 509-519.

[28] **Kaur, M., & Srivastava, A. K.** (2002). Photopolymerization: A review. *Journal of Macromolecular Science, Part C: Polymer Reviews*, *42*(4), 481-512.

[29] **Yagci, Y., & Hepuzer, Y.** (1999). A novel visible light initiatiating system for cationic polymerization. *Macromolecules*, *32*(19), 6367-6370.

[30] **Green, W. A.** (2010). Industrial photoinitiators: a technical guide. CRC Press.

[31] **Schofield, J. D.** (2002). Extending the boundaries of dispersant technology. *Progress in Organic Coatings*, *45*(2-3), 249-257.

[32] **& Crivello, J. V.** (2005). Investigation of the Reactivity of Epoxide Monomers in Photoinitiated Cationic Polymerization, Macromolecules, 38(9), 3584–3595.

[33] **Kahveci, M. U., Tasdelen, M. A., & Yagci, Y.** (2007). Photochemically initiated free radical promoted living cationic polymerization of isobutyl vinyl ether, Polymer, 48(8), 2199–2202.

[34] **Puskas, J. E., Michel, A., & Barghi, S.** (1999). Ionic Polymerizations and Related Processes, NATO Science Series, 369.

[35] **Ligon-Auer, S. C., Schwentenwein, M., Gorsche, C., Stampfl, J., & Liska, R.** (2016). Toughening of photo-curable polymer networks: a review. *Polymer Chemistry*, *7*(2), 257-286.

[36] **Lapin, S. C., Snyder, J. R., Sitzmann, E. V., Barnes, D. K., & Green, G. D.** (1995). *U.S. Patent No. 5,437,964*. Washington, DC: U.S. Patent and Trademark Office.

[37] **Xu, J**. Photo-Curable Resin Composition. U.S. Patent 9090020, 2015.

[38] **Yamamura, T., Watanabe, T., Takeuchi, A., & Ukachi, T.** (2002). *U.S. Patent No. 6,365,644*. Washington, DC: U.S. Patent and Trademark Office.

[39] **Al Mousawi, A., Dumur, F., Garra, P., Toufaily, J., Hamieh, T., Goubard, F., ... & Lalevée, J.** (2017). Azahelicenes as visible light photoinitiators for cationic and radical polymerization: Preparation of photoluminescent polymers and use in high performance LED projector 3D printing resins. *Journal of Polymer Science Part A: Polymer Chemistry*, *55*(7), 1189-1199.

[40] **Sangermano, M.** (2012). Advances in cationic photopolymerization, Pure and Applied Chemistry, 84(10), 2089–2101.

[41] **Crivello, J. V. (**1983). Cationic polymerization: Iodonium and sulfonium salt photoinitiators. Initiators, 1–48.

[42] **Crivello, J. V.** (1999). The discovery and development of onium salt cationic photoinitiators. Journal of Polymer Science Part A: Polymer Chemistry, 37(23), 4241–4254.

[43] **Toba, Y., Saito, M., & Usui, Y.** (1999). Cationic Photopolymerization of Epoxides by Direct and Sensitized Photolysis of Onium Tetrakis(pentafluorophenyl)borate Initiators, Macromolecules, 32(10), 3209–3215.

[44] **Yagci, Y., Durmaz, Y. Y., & Aydogan, B.** (2007). Phenacyl onium salt photoinitiators: synthesis, photolysis, and applications, The Chemical Record, 7(2), 78–90.

[45] **Villotte, S., Gigmes, D., Dumur, F., & Lalevée, J.** (2019). Design of Iodonium Salts for UV or Near-UV LEDs for Photoacid Generator and Polymerization Purposes, Molecules, 25(1), 149.

[46] **Crivello, J.** (2015). Sensitization of Cationic Photopolymerizations, Dyes and Chromophores in Polymer Science, 45–79.

[47] **Nurchi, C., Buonvino, S., Arciero, I., & Melino, S.** (2023). Sustainable Vegetable Oil-Based Biomaterials: Synthesis and Biomedical Applications. *International Journal of Molecular Sciences*, *24*(3), 2153.

[48] **Sperling, L. H.** (2012). *Interpenetrating polymer networks and related materials*. Springer Science & Business Media.

[49] **Sperling LH, Mishra V. In:** (1996) Salomone JC, editor. Polymer materials encyclopedia, vol. 5. New York: CRC Press, 1996. p. 3292.

[50] **Konuray, O., Fernández-Francos, X., Ramis, X., & Serra, À. (**2018). State of the art in dual-curing acrylate systems. *Polymers*, *10*(2), 178.

[51] **Redmann, A., & Osswald, T. A.** (2021). A model for modulus development of dual-cure resin systems. *Polymer Engineering & Science*, *61*(3), 830-835.

[52] **Decker, C., Viet, T. N. T., Decker, D., & Weber-Koehl, E.** (2001). UV-radiation curing of acrylate/epoxide systems. *Polymer*, *42*(13), 5531-5541.

[53] **Park, C. H., Lee, S. W., Park, J. W., & Kim, H. J.** (2013). Preparation and characterization of dual curable adhesives containing epoxy and acrylate functionalities. *Reactive and Functional Polymers*, *73*(4), 641-646.

[54] **Bednarczyk, P., Mozelewska, K., Nowak, M., & Czech, Z.** (2021). Photocurable Epoxy Acrylate Coatings Preparation by Dual Cationic and Radical Photocrosslinking. *Materials*, *14*(15), 4150.

[55] **Tanurdjaja, S., Tallon, C., Scales, P. J., & Franks, G. V.** (2011). Influence of dispersant size on rheology of non-aqueous ceramic particle suspensions. *Advanced Powder Technology*, *22*(4), 476-481.

[56] **Nowers, J. R., & Narasimhan, B.** (2006). The effect of interpenetrating polymer network formation on polymerization kinetics in an epoxy-acrylate system. *Polymer*, *47*(4), 1108-1118.

[57] **Silverstein, M. S.** (2020). Interpenetrating polymer networks: So happy together?. Polymer, 207, 122929.

[58] **Ramis, X., Fernández-Francos, X., De la Flor, S., Ferrando, F., & Serra, À.** (2018). Click-based dual-curing thermosets and their applications. In *Thermosets* (pp. 511-541). Elsevier.

[59] **Amerio, E., Sangermano, M., Malucelli, G., Priola, A., & Voit, B.** (2005). Preparation and characterization of hybrid nanocomposite coatings by photopolymerization and sol–gel process. *Polymer*, *46*(25), 11241-11246.

[60] **Alamán, J., López-Valdeolivas, M., Alicante, R., Medel, F. J., Silva-Treviño, J., Peña, J. I., & Sánchez-Somolinos, C.** (2018). Photoacid catalyzed organic–inorganic hybrid inks for the manufacturing of inkjet-printed photonic devices. *Journal of Materials Chemistry C*, *6*(15), 3882-3894.

[61] **Wu, Y., Su, H., Li, M., & Xing, H.** (2022). Digital light processing-based multi-material bioprinting: Processes, applications, and perspectives. *Journal of Biomedical Materials Research Part A*.

[62] **Fernández-Francos, X., Konuray, O., Ramis, X., Serra, À., & De la Flor, S.** (2020). Enhancement of 3D-printable materials by dual-curing procedures. *Materials*, *14*(1), 107.

[63] **Liu, P., Gu, A., Liang, G., Guan, Q., & Yuan, L.** (2012). Preparation and properties of novel high performance UV-curable epoxy acrylate/hyperbranched polysiloxane coatings. *Progress in Organic Coatings*, *74*(1), 142-150.

[64] **Asif, A., Huang, C., & Shi, W.** (2004). Structure–property study of waterborne, polyurethane acrylate dispersions based on hyperbranched aliphatic polyester for UV-curable coatings. *Colloid and polymer science*, *283*(2), 200-208.

[65] **Sun, J., Binner, J., & Bai, J.** (2019). Effect of surface treatment on the dispersion of nano zirconia particles in non-aqueous suspensions for stereolithography. *Journal of the European Ceramic Society*, *39*(4), 1660-1667.

[66] **Hoyle, C. E.; Lee, T. Y.; Roper, T. Thiol-Enes**: Chemistry of the Past with Promise for the Future. J. Polym. Sci., Part A: Polym. Chem. 2004, 42, 5301– 5338, DOI: 10.1002/pola.20366

[67] **Husár, B., Ligon, S. C., Wutzel, H., Hoffmann, H., & Liska, R.** (2014). The formulator's guide to anti-oxygen inhibition additives. *Progress in Organic Coatings*, *77*(11), 1789-1798.

[68] **McNair, O. D., Janisse, A. P., Krzeminski, D. E., Brent, D. E., Gould, T. E., Rawlins, J. W., & Savin, D. A.** (2013). Impact properties of thiol–ene networks. *ACS applied materials & interfaces*, *5*(21), 11004-11013.

[69] **Oesterreicher, A., Wiener, J., Roth, M., Moser, A., Gmeiner, R., Edler, M., ... & Griesser, T.** (2016). Tough and degradable photopolymers derived from alkyne monomers for 3D printing of biomedical materials. *Polymer Chemistry*, *7*(32), 5169-5180.

[70] **Wu, Y., Simpson, M. C., & Jin, J. (**2022). 3D Printing of Thiol-Yne Photoresins through Visible Light Photoredox Catalysis. ChemistrySelect, 7(10), e202200319.

[71] **Pandey, R.** (2014). Photopolymers in 3D printing applications.

[72] **Zakeri, S., Vippola, M., & Levänen, E.** (2020). A comprehensive review of the photopolymerization of ceramic resins used in stereolithography. *Additive Manufacturing*, *35*, 101177.

[73] **Tomeckova, V., & Halloran, J. W.** (2010). Cure depth for photopolymerization of ceramic suspensions. *Journal of the European Ceramic Society*, *30*(15), 3023-3033.

[74] **Goswami, A., Ankit, K., Balashanmugam, N., Umarji, A. M., & Madras, G.** (2014). Optimization of rheological properties of photopolymerizable alumina suspensions for ceramic microstereolithography. *Ceramics International*, *40*(2), 3655-3665.

[75] **Ertugrul., C., Hassel., E.,** (2020) 3D Printing Method for "Global Materials Management" Process.

[76] **Seo, D. C., Lee, J. J**. (1995). Effect of embedded optical fiber sensors on transverse crack spacing of smart composite structures. Composite Structures, 32, 51-58. doi: 10.1016/0263-8223(95)00039-9.

[77] **ÖZBAY, B.** (2021). ISTANBUL TECHNICAL UNIVERSITY★ GRADUATE SCHOOL.Griffith, M. L., & Halloran, J. W. (1996). Freeform fabrication of ceramics via stereolithography. *Journal of the American Ceramic Society*, *79*(10), 2601-2608.

[78] **Johansson, E., Lidström, O., Johansson, J., Lyckfeldt, O., & Adolfsson, E.** (2017). Influence of resin composition on the defect formation in alumina manufactured by stereolithography. *Materials*, *10*(2), 138.

[79] **Bártolo, P. J. (Ed.). (**2011). *Stereolithography: materials, processes and applications*. Springer Science & Business Media.

[80] **Eshkalak, S.K., Ghomi, E.R., Dai, Y., Choudhury, D., Ramakrishna, S.** (2020). The role of three-dimensional printing in healthcare and medicine. Materials & Design, 108940.

[81] **Melchels, F.P., Feijen, J., Grijpma, D.W.** (2010). A review on stereolithography and its applications in biomedical engineering. Biomaterials, 31 (24), 6121-6130

[82] **Devi, L., Gaba, P., Chopra, H.** (2019). Tailormade Drug Delivery System: A Novel Trio Concept of 3BP+ Hydrogel+ SLA. Journal of Drug Delivery and Therapeutics, 9 (4-s), 861-866.

[83] **Bove, A., Calignano, F., Galati, M., & Iuliano, L.** (2022). Photopolymerization of ceramic resins by stereolithography process: a review. *Applied Sciences*, *12*(7), 3591.

[84] **Zhu, W., Qu, X., Zhu, J., Ma, X., Patel, S., Liu, J., ... & Chen, S.** (2017). Direct 3D bioprinting of prevascularized tissue constructs with complex microarchitecture. *Biomaterials*, *124*, 106-115.

[85] **Yang, Y., Zhou, Y., Lin, X., Yang, Q., & Yang, G.** (2020). Printability of external and internal structures based on digital light processing 3D printing technique. *Pharmaceutics*, *12*(3), 207.

[86] **Hopkinson, N., & Dickens, P.** (2006). Emerging rapid manufacturing processes. *Rapid manufacturing: an industrial revolution for the digital age*, 55-80.

[87] **Depboylu., F., Dalgarno., K., (**2017). 3D Prıntıng porous polymer structures for tıssue engıneerıng.

[88] **Oezkan, B., Sameni, F., Karmel, S., Engstrøm, D. S., & Sabet, E. (**2021). A systematic study of vat-polymerization binders with potential use in the ceramic suspension 3D printing. *Additive Manufacturing*, *47*, 102225.

[89] **de Camargo, I. L., Morais, M. M., Fortulan, C. A., & Branciforti, M. C**. (2021). A review on the rheological behavior and formulations of ceramic suspensions for vat photopolymerization. *Ceramics International*, *47*(9), 11906-11921.

[90] **Truxova, V. E. R. O. N. I. K. A., Safka, J. I. R. I., Seidl, M. A. R. T. I. N., Kovalenko, I. A. R. O. S. L. A. V., Volesky, L. U. K. A. S., & Ackermann, M. I. C. H. A. L.** (2020). Ceramic 3D printing: Comparison of SLA and DLP technologies. MM Sci. J, 2020, 3905-3911.

CURRICULUM VITAE

Name Surname **:** İrem Şeyma ÖZBALAK

EDUCATION

- **B.Sc.** **:** 2018, Marmara University, Faculty of Science and Literature, Chemistry Department
- **M.Sc.** **:** 2019, Istanbul Technical University, Department of Polymer Science and Technology, Polymer Science and Technology Programme

PROFESSIONAL EXPERIENCE AND REWARDS:

- 2018, Contract Faux Leather Limited Company, Summer Intern
- 2020-2021, Production Development Assistant Specialist, Özak Textile
- 2022-2023, TÜBİTAK MAM, Project Scholarship